Int J Earth Sci (Geol Rundsch) (2017) 106:1665–1692
DOI 10.1007/s00531-016-1380-6

ORIGINAL PAPER

Evidence of Variscan and Alpine tectonics in the structural and thermochronological record of the central Serbo-Macedonian Massif (south-eastern Serbia)

Milorad D. Antić[1] · Alexandre Kounov[1] · Branislav Trivić[2] · Richard Spikings[3] · Andreas Wetzel[1]

Received: 29 February 2016 / Accepted: 12 July 2016 / Published online: 27 July 2016

Abstract The Serbo-Macedonian Massif (SMM) represents a composite crystalline belt within the Eastern European Alpine orogen, outcropping from the Pannonian basin in the north to the Aegean Sea in the south. The central parts of this massif (south-eastern Serbia) consist of the medium- to high-grade Lower Complex and the low-grade Vlasina Unit. Outcrop- and micro-scale ductile structures in this area document three major stages of ductile deformation. The earliest stage D_1 is related to isoclinal folding, commonly preserved as up to decimetre-scale quartz–feldspar rootless fold hinges. D_2 is associated with general south-eastward tectonic transport and refolding of earlier structures into recumbent metre- to kilometre-scale tight to isoclinal folds. Stages D_1 and D_2 could not be temporally separated and probably took place in close sequence. The age of these two ductile deformation stages was constrained to the Variscan orogeny based on indirect geological evidence (i.e. ca. 408-ca. 328). During this period, the SMM was involved in a transpressional amalgamation of the western and eastern parts of the Galatian super-terrane and subsequent collision with Laurussia. Outcrop-scale evidence of the final stage D_3 is limited to spaced and crenulation cleavage, which are probably related to formation of large-scale open upright folds as reported previously. $^{40}Ar/^{39}Ar$ thermochronology was applied on hornblende, muscovite, and biotite samples in order to constrain the age of tectonothermal events and activity along major shear zones. These $^{40}Ar/^{39}Ar$ data reveal three major cooling episodes affecting the central SMM. Cooling below greenschist facies conditions in the western part of the Vlasina Unit took place in a post-orogenic setting (extensional or transtensional) in the early Permian (284 ± 1 Ma). The age of activity along the top-to-the-west shear zone formed within the orthogneiss in the Božica area of the Vlasina Unit was constrained to Middle Triassic (246 ± 1 Ma). This age coincides with widespread extension related to the opening of the Mesozoic Tethys. The greenschist facies retrogression in the Lower Complex probably occurred in the Early Jurassic (195 ± 1 Ma), and it was related to the thermal processes in the overriding plate above the subducting slab of the Mesozoic Tethys Ocean.

Keywords Serbo-Macedonian Massif · Ductile deformation · $^{40}Ar/^{39}Ar$ thermochronology · Variscan orogeny · Serbia

Introduction

Crystalline terranes within the Eastern Mediterranean Alpine orogen (e.g. Tisza, Pelagonia, Rhodope, Serbo-Macedonian Massif) commonly display a high degree of structural complexity resulting from the interplay between inherited structures and variable amount of Alpine deformational overprint (e.g. Dimitrijević 1972; Stampfli et al. 2002; Neubauer 2002; von Raumer et al. 2003, 2013; Burg

Electronic supplementary material The online version of this article (doi:10.1007/s00531-016-1380-6) contains supplementary material, which is available to authorized users.

✉ Milorad D. Antić
m.antic@unibas.ch

[1] Institute for Geology and Palaeontology, University of Basel, 4056 Basel, Switzerland

[2] Faculty of Mining and Geology, University of Belgrade, Belgrade 11000, Serbia

[3] Section des Sciences de la Terre et de l'Environnement, Université de Genève, 1205 Geneva, Switzerland

2012). These basement units usually represent segments of the North-Gondwanan margin that drifted along multiple branching oceanic domains and subsequently accreted to the Eurasian margin during the Variscan orogeny (e.g. Neubauer 2002; Karamata 2006; Stampfli et al. 2013). A similar evolution took place again during the Alpine orogeny with polyphase opening of the Mesozoic Tethys and its consequent closure involving collision of multiple crustal segments (e.g. Robertson et al. 1991; Ricou 1994; Schmid et al. 2008; Stampfli and Hochard 2009). Therefore, to reveal the tectonic evolution of these intra-Alpine crystalline units, their complex structural patterns need to be studied in detail together with determination of age of their protoliths and timing of metamorphism.

The crystalline Serbo-Macedonian Massif (SMM; Dimitrijević 1957) is lodged between the Dinaride and the Carpatho-Balkanide chains of the Alpine orogen (Fig. 1). Paucity of structural, geo-, and thermochronological data has led to a number of contrasting tectonic interpretations and structural subdivisions within the SMM (Popović 1991, 1995; Ricou et al. 1998; Grubić et al. 1999, 2005; Kräutner and Krstić 2002; Zagorchev and Milovanović 2006). A similar degree of uncertainty also plagued the neighbouring Rhodope metamorphic complex, until its tectonic evolution was re-evaluated using combined detailed structural and geochronological studies (e.g. Burg et al. 1995; Mukasa et al. 2003; Peytcheva et al. 2004; Liati 2005; Bosse et al. 2009; Bonev et al. 2010, 2015; Turpaud and Reischmann 2010; Jahn-Awe et al. 2010, 2012; Himmerkus et al. 2011; Froitzheim et al. 2014; Georgiev et al. 2016). Detailed reconstructions of the tectonic evolution of areas surrounding the SMM (i.e. Southern Carpathians, Internal Dinarides) have also been recently produced based on reliable data sets (Dallmeyer et al. 1998; Matenco and Schmid 1999; Fügenschuh and Schmid 2005; Schmid et al. 2008; Ustaszewski et al. 2009; Zelic et al. 2010; Stojadinovic et al. 2013; Toljić et al. 2013). Furthermore, recent detailed studies in the southern part of the SMM (i.e. Vertiskos Unit in Greece) have provided valuable constraints on the magmatic and deformation events that affected this unit (e.g. Himmerkus et al. 2009a, b; Meinhold et al. 2010; Kydonakis et al. 2014, 2015a, b). Due to its particular position between the two divergent belts of the Alpine orogen, unravelling of thermal and deformation history of the SMM becomes essential for correct reconstruction of the evolution of tectonic units in south-eastern Europe. The central parts of the SMM (south-eastern Serbia) were chosen for this study due to relative scarcity of reliable data and relatively good condition of rock exposures. This study provides new detailed structural data and $^{40}Ar/^{39}Ar$ thermochronology results from the central SMM, which were used to unravel its long and complex deformation history since the Palaeozoic.

Geological setting

The SMM represents a crystalline belt outcropping from the Pannonian basin in the north to the Aegean Sea in the south (Fig. 1). It should be noted that although our study concerns both Variscan and Alpine tectonics in the SMM, the names of the tectonic units discussed below only refer to the later (i.e. Alpine) tectonics so that results presented here could be correlated with the previously published tectonic frameworks of south-eastern Europe. The Supragetic nappe sequence of the South Carpathians is considered to be the continuation of the SMM east and north-east of the Pannonian basin (Săndulescu 1984; Dimitrijević 1997; Schmid et al. 2008). As originally proposed by Dimitrijević (1957), the SMM in Serbia comprises a structurally lower (the Lower Complex) and upper unit (Vlasina Unit). These are commonly distinguished by their metamorphic grade, i.e. the Lower Complex underwent medium- to

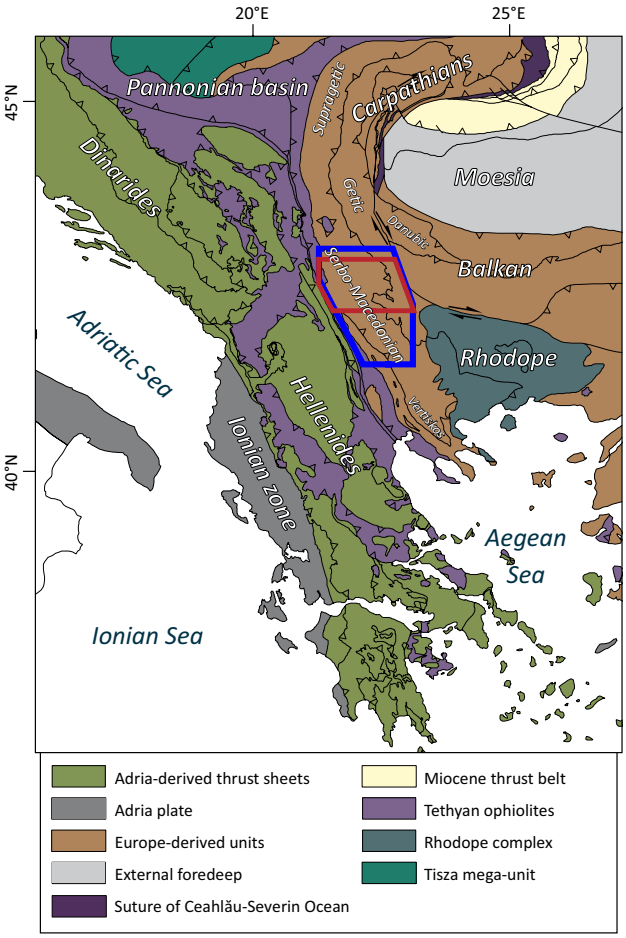

Fig. 1 Tectonic map of the Balkan Peninsula (modified after Schmid et al. 2008; van Hinsbergen and Schmid 2012). *Blue polygon* outlines the area of the map in Fig. 2, and the *red polygon* in Fig. 3

lower-amphibolite facies metamorphism, whereas the Vlasina Unit was metamorphosed at greenschist facies conditions. In Bulgaria, the continuations of the Lower Complex and the Vlasina Unit are referred to as the Ograzhden Unit (Dimitrijević 1967; Zagorchev 1984; Dabovski et al. 2002) and Morava Unit (e.g. Zagorchev 1985, 1993), respectively. The SMM can be followed farther southwards into Greece, where the Vertiskos unit is usually correlated with rocks of the Lower Complex (Kockel et al. 1971; Burg et al. 1995; Himmerkus et al. 2006, 2009a). However, only the central parts of the SMM (south-eastern Serbia) were investigated during this study.

Lower Complex

The Lower Complex consists mainly of gneisses, micaschists, quartzites, amphibolites, and occasionally marbles and migmatites (Dimitrijević 1963). These rocks represent a Cadomian (late Neoproterozoic–earliest Cambrian) volcano-sedimentary complex developed along the active margin of north Gondwana, which was subsequently intruded by igneous rocks during several magmatic pulses (Antić et al. 2015a, b). Although medium- to lower-amphibolite facies metamorphism is characteristic for the Lower Complex (Dimitrijević 1967; Milovanović 1990, 1992; Cvetković 1992), relicts of eclogite facies rocks are also reported as isolated occurrences throughout this unit (Balogh et al. 1994; Iancu et al. 1998; Korikovsky et al. 2003; Zidarov et al. 2003a; Macheva et al. 2005; Nenova and Zidarov 2008; Ivanova and Zidarov 2011; Kydonakis et al. 2015b). The timing of high-pressure (HP) metamorphism, deduced from overprinting relationships and whole-rock Rb/Sr data, was reported to be of pre-Cadomian or Cadomian age (ca. 750-550 Ma), with an amphibolite facies overprint and locally migmatisation occurring in the Variscan (Dimitrijević 1967; Balogh et al. 1994; Zagorchev and Milovanović 2006; Nenova and Zidarov 2008; Peytcheva et al. 2009a; Antić et al. 2015b). Additionally, U–Pb dating of titanite and several K/Ar analyses have yielded Early Cretaceous ages (Milovanović 1990; Balogh et al. 1994; Zidarov et al. 2003b).

Vlasina Unit

The Vlasina Unit represents a Cadomian volcano-sedimentary sequence, which, although similar to the protoliths of the Lower Complex, is generally dominated by ocean-floor sediments (Pantić et al. 1967; Petrović 1969), intruded by late Cadomian igneous rocks (Antić et al. 2015b), covered by a Lower Ordovician to lower Carboniferous sedimentary sequence (post-Cambrian in Fig. 2; Pavlović 1962; Babović et al. 1977; Kräutner and Krstić 2002), and finally intruded by late Palaeogene magmatic rocks (Antić et al. 2015a). The pre-Ordovician Vlasina (Antić et al. 2015b) is typically represented by various schists, phyllites, and quartzites (Dimitrijević 1967). Peak metamorphic conditions of 450–500 °C at 3–5 kbar (0.3–0.5 GPa) were reported in the pre-Ordovician Vlasina (Milovanović et al. 1988; Vasković 2002). However, relicts of metamorphic assemblages indicative of conditions exceeding greenschist facies have been reported in the vicinity of the Božica magmatic complex and Vranjska Banja area (Fig. 2; Petrović 1969, 1977; Vujanović et al. 1974; Babović et al. 1977; Vasković 1998; Vasković et al. 2003).

Post-Cambrian Vlasina (Antić et al. 2015b) comprises Ordovician schists, phyllites, calcschists, argillites, quartzite and marbles, Silurian graptolitic schists, Middle Devonian carbonates and argillites, and Upper Devonian to lower Carboniferous turbidites with spilites (Pavlović 1962, 1977; Petrović et al. 1973; Spassov 1973; Babović et al. 1977; Zagorčev and Bončeva 1988; Banjac 2004; Lakova 2009). These rocks are considered to have experienced very-low-grade metamorphism with only occasional occurrences of greenschist facies assemblages (Petrović et al. 1973; Spassov 1973; Babović et al. 1977; Graf 2001; Krstić et al. 2002).

The tectonic contact of the Lower Complex with the Vlasina Unit is reported as the Vrvi Kobila shear zone (Fig. 2). It was previously considered as a pre-Mesozoic west-vergent thrust juxtaposing the Vlasina Unit over the Lower Complex (Vukanović et al. 1973; Krstić and Karamata 1992), or, alternatively, as a post-Late Cretaceous dextral shear zone (Kräutner and Krstić 2002). Additionally, several reports suggest that these units originally had a stratigraphic contact, which was later tectonically reworked (Petrović and Karamata 1965; Petrović 1969; Dimitrijević 1997).

Eastern Veles series

South-west of Bujanovac (Fig. 2), the Lower Complex overlies the eastern part of the Veles series. This contact was previously considered as a strike-slip fault (Malešević et al. 1980; Vukanović et al. 1982), an east-vergent thrust (Krstić and Karamata 1992), or a westward thrust reactivated as dextral strike slip in the Neogene (Kräutner and Krstić 2002). It has been recently interpreted as a ductile shear zone (Stefan M. Schmid, personal communication, September 2014), along which no significant vertical movement occurred since the Late Cretaceous (Antić et al. 2015a). Jurassic ophiolites of the Eastern Vardar oceanic domain together with the Upper Cretaceous flysch (Vukanović et al. 1977; Pavić et al. 1983; Karamata and Krstić 1996) divide the Veles series into eastern and western part. The Eastern Veles series (EVS) is largely composed of a lower Palaeozoic sedimentary sequence and

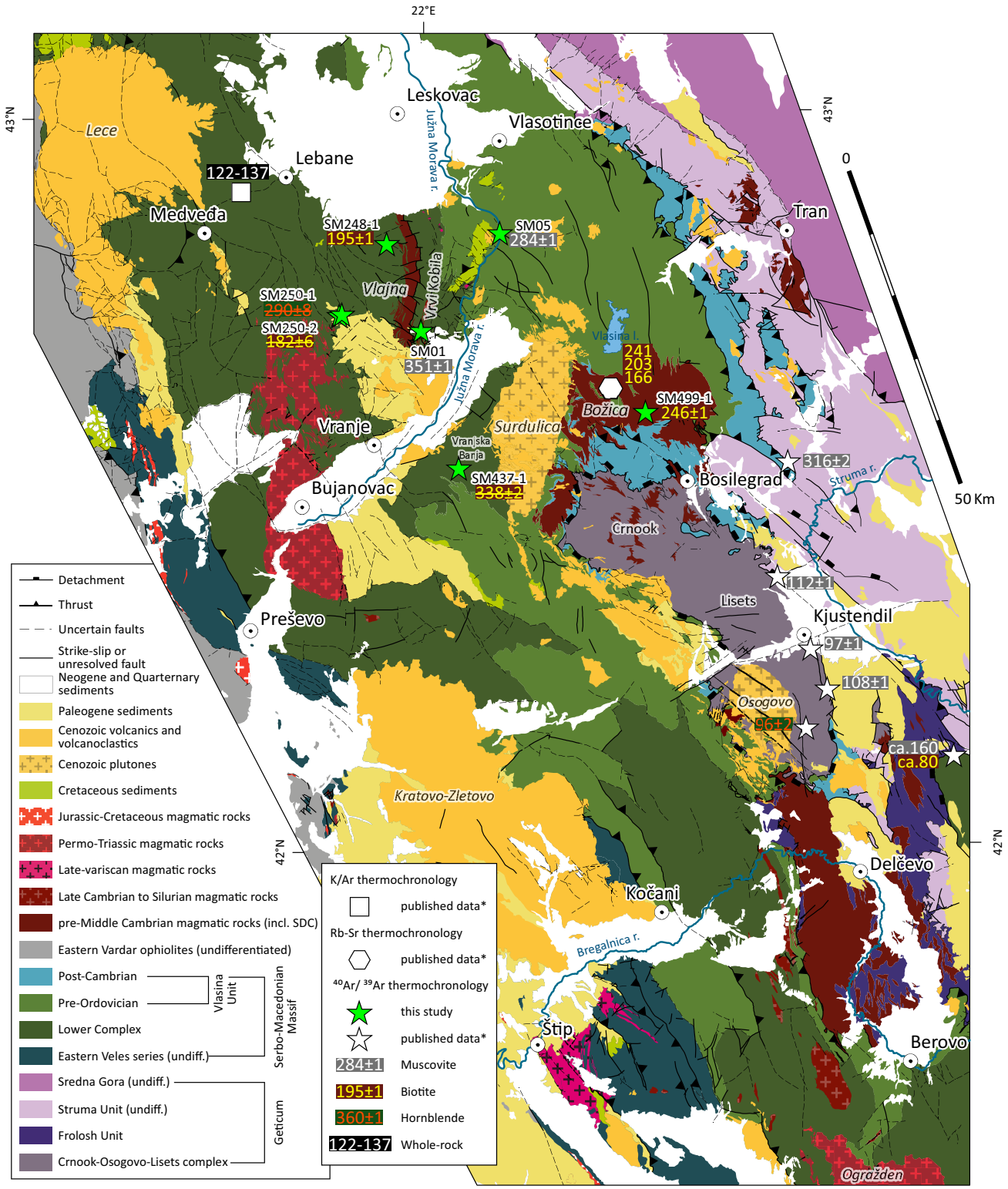

Fig. 2 Tectonic map of the study area with the sampling locations and results of $^{40}Ar/^{39}Ar$ thermochronology (after basic geological maps of SFR Yugoslavia 1:1,000,000 and geological maps of Bulgaria 1:100,000 and 1:50,000). Labels in a regular type represent toponyms, whereas labels in an *italic type* represent igneous complexes. *Asterisk* Literature data from Babović et al. (1977), Milovanović (1990), Kounov (2002), and Kounov et al. (2010). Striken-through dates are related to the $^{40}Ar/^{39}Ar$ analyses with no reliable plateau dates. See text for details

Early Ordovician meta-granites (Pavlović 1977; Antić et al. 2015b), with minor Triassic sedimentary cover (Pavić et al. 1983). These rocks underwent amphibolite facies metamorphism, followed by a post-Triassic intensive retrogression in greenschist facies (Dimitrijević 1997). In contrast, Devonian to Triassic greenschist facies meta-sedimentary rocks constitute the majority of the Western Veles series (Pavić et al. 1983; Grubić and Ercegovac 2002). The Veles series is considered to be a part of the Circum-Rhodope belt (Zagorchev and Milovanović 2006; Schmid et al. 2008), or the "internal Vardar zone" (Dimitrijević and Drakulić 1958; Robertson et al. 2009). This study only addresses the lower Palaeozoic-dominated EVS, which was recently attributed to the Palaeozoic Galatian supra-terrane together with the SMM (Antić et al. 2015b).

Struma unit and Crnook–Osogovo–Lisets complex

During the late Early Cretaceous, the Vlasina Unit was thrust to the east onto the Struma and other Getic units along a system of east- to north-east-vergent thrusts (Petković 1930; Mihailescu et al. 1967; Petrović 1969; Zagorchev and Ruseva 1982; Lilov and Zagorchev 1993; Kounov et al. 2010). The Struma Unit consists of a basement represented by variably deformed continent- and ocean-derived rocks of Ediacaran to early Cambrian age (Kounov et al. 2012), and a transgressive Permian to Lower Cretaceous sedimentary cover (Zagorchev 1981).

The Crnook–Osogovo–Lisets (COL) complex in south-eastern part of the study area represents an extensional dome exhumed from below Struma and Vlasina Units during middle Eocene to Oligocene (Kounov et al. 2004; Antić et al. 2015a). It consists of micaschists, gneisses, amphibolites, and quartzites (Dimitrova 1964; Dimitrijević 1972; Babović et al. 1977). Magmatic rocks of the COL complex and the basement of Struma Unit are derived from the same calc-alkaline magma source associated with a magmatic-arc complex formed during Ediacaran to early Cambrian (Kounov et al. 2012; Antić et al. 2015b). These rocks have experienced lower-amphibolite facies metamorphism during an early Late Cretaceous compressional event (Kounov et al. 2010).

Sedimentary cover and brittle tectonics

The oldest undeformed and non-metamorphosed rocks in the study area are the Santonian to lower Maastrichtian sedimentary rocks (86–70 Ma, Fig. 2). These relatively shallow Late Cretaceous basins were filled with predominantly terrigenous clastic deposits with subordinate marls and limestones (Petrović et al. 1973). Palaeogene sedimentary rocks in the area are represented by middle Eocene carbonate continental deposits (Petrović et al. 1973; Vukanović et al. 1973; Anđelković and Anđelković 1995), upper Eocene turbidites (Vukanović et al. 1977; Dimitrijević and Dimitrijević 1987), and Oligocene marine to lacustrine sedimentary rocks (Vukanović et al. 1973, 1977) deposited in extensional basins that were coeval with the exhumation of the COL core complex. Palaeogene sedimentary rocks are often intercalated with various pyroclastic rocks or intruded by small dacitic or andesitic bodies that also intrude the basement. The most prominent igneous complexes in the study area are the Surdulica granodiorite (Antić et al. 2015a), and the Lece andesitic complex (Karamata et al. 1992).

Neogene sedimentary rocks in the area are represented by middle Miocene clastic deposits and freshwater marls, which were continually deposited during the Pliocene (Vukanović et al. 1973, 1977). These rocks are intercalated with dacitic and andesitic volcanoclastic rocks (Vukanović et al. 1977).

Apart from the Early Cretaceous compression discussed above, brittle deformation in central SMM also includes Late Cretaceous normal faulting, Eocene–Oligocene extension (Antić et al. 2015a), and dextral strike-slip and oblique faulting during Miocene to recent wrench tectonics (Petrović 1969; Marović et al. 2007; Burchfiel et al. 2008; Kounov et al. 2011; Tranos and Lacombe 2014; Mladenović et al. 2014).

Structural data

No coherent ductile fabric could be followed throughout the entire study area (i.e. central SMM), as abrupt changes in orientation of structural elements occur even within relatively small areas (Fig. 3). These changes are considered to result from a much younger brittle tectonic overprint. The structural observations were hampered further by generally poor exposure and highly weathered state of rocks in the study area. Despite these difficulties, three major stages of ductile deformation affecting the entire study area were identified based on overprinting relationships and internal geometries of the resulting structures (i.e. style of deformation).

Lower Complex

Due to complex structural patterns, the deformation in the Lower Complex will be described in five separate domains that display some degree of structural homogeneity (Fig. 4).

Western part of the Lower Complex

The area west of the brittle Tupale fault is characterised by a predominantly east-dipping main foliation S_2, which represents the axial-plane cleavage of overturned to recumbent

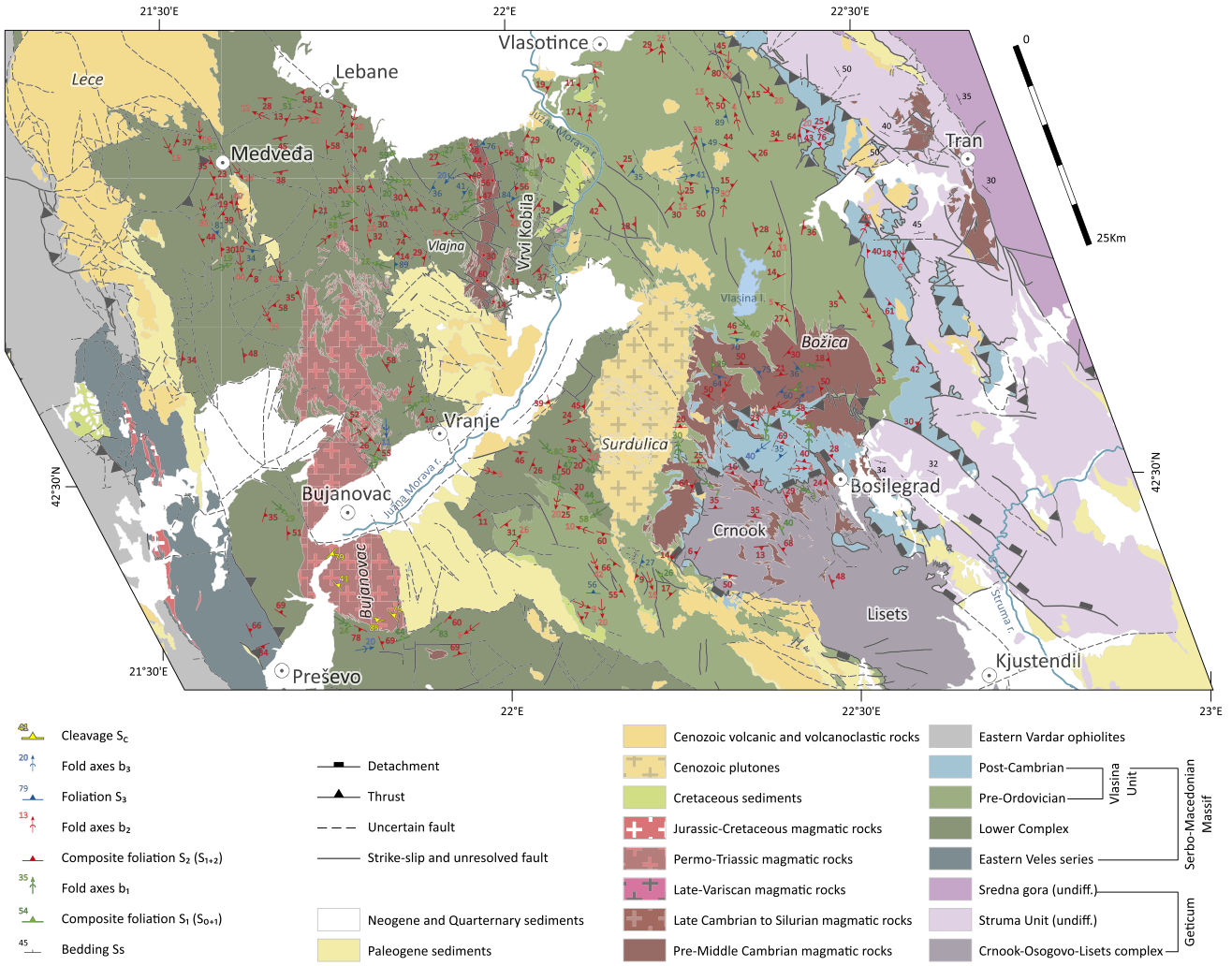

Fig. 3 Tectonic map of the study area with structural elements (after basic geological maps of SFR Yugoslavia 1:1,000,000 and geological maps of Bulgaria 1:100,000 and 1:50,000). Labels in *regular type* represent toponyms, whereas labels in *italic type* represent igneous complexes

metre- to kilometre-scale isoclinal F_2 folds (Fig. 4a). Fold axes b_2 are shallowly plunging in the north to north-west–south to south-east direction (Figs. 4a, 5a), and are generally perpendicular to subhorizontal fold axes b_1 of earlier folds F_1 (Fig. 4a). Refolding of decimetre-scale isoclinal F_1 folds (i.e. folded quartz-feldspar bands with fold axis b_1 perpendicular to the plane of image in Fig. 5b), by isoclinal folds F_2 at high to almost right angles (parallel to the plane of image in Fig. 5b) has been observed at several outcrops. Therefore, an earlier foliation (S_i) is presumed to be initially folded into F_1 and subsequently refolded into F_2 folds. Away from the hinges of F_2 folds, the supposed initial foliation S_i and foliation S_1 formed during D_1 were completely transposed during D_2 such that the main fabric represents a $S_i/S_1/S_2$ composite foliation, which is designated as S_2 for convenience. Apart from the rare outcrops where the relationships between folds F_1 and F_2 could be directly observed, the early folds F_1 are usually found as rootless fold hinges in the microlithons bound by foliation S_2. A clear distinction between fold structures related to deformation stages D_1 and D_2 is only possible in areas where their respective fold axes intersect at high angles.

A younger spaced cleavage S_3 is usually perpendicular or at a high angle to S_2, and generally strikes north-west–south-east (Fig. 4a).

A subhorizontal stretching lineation defined by biotite and elongated quartz-feldspar aggregates trends north to north-east–south to south-west (Fig. 4a). Polycrystalline sigmoids and δ-type aggregates observed in *XZ* planes at two locations indicate a top-to-the-north to north-east and a top-to-the-south sense of shear (Fig. 6).

Central part of the Lower Complex

A relatively large area in the central part of the Lower Complex is characterised by predominantly shallow dipping

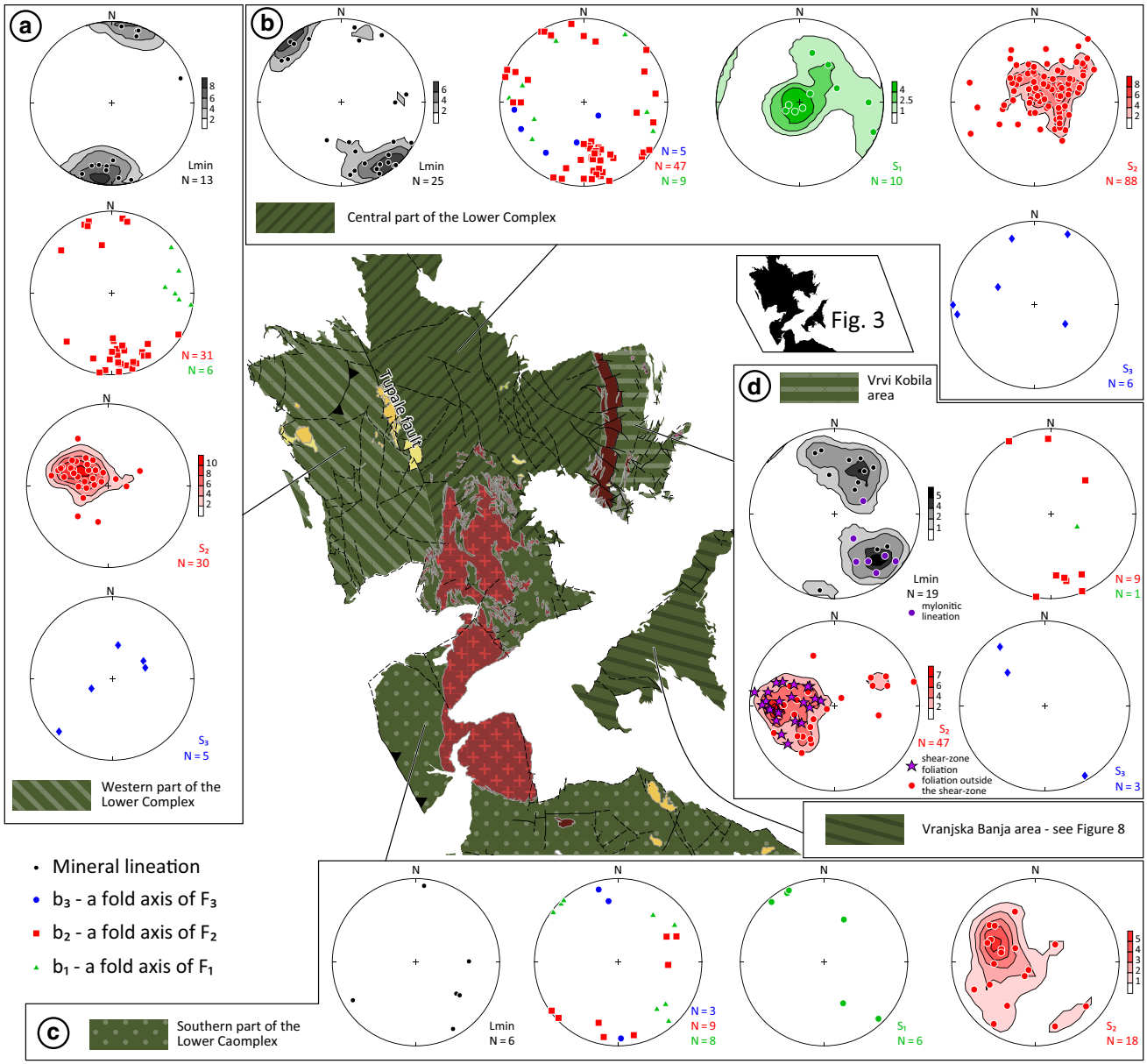

Fig. 4 Lower hemisphere equal-area plots of structural elements from **a** western part of the Lower Complex, **b** central part of the Lower Complex, **c** southern part of the Lower Complex, and **d** Vrvi Kobila area. For structural data in Vranjska Banja area, please see Fig. 8. *Inset* shows the relative scale and position in Fig. 3

penetrative foliation with a preferred dip direction in the south-western quadrant (S_2; Fig. 4b). This fabric is predominantly formed by flattened quartz–feldspar aggregates and biotite. The earlier foliation S_1 is preserved only at the hinges of large-scale (Dm to km) isoclinal recumbent folds F_2. In these hinge zones, S_1 is often folded into metre-size parasitic F_2 folds, whereas S_2 represents the axial-plane cleavage. As the foliation S_1 was observed only at hinges of folds F_2, its statistical distribution (Fig. 4b) reflects the geometry of limbs of large recumbent folds F_2. The subhorizontal maximum of S_1 is related to the shallow inclination of one of the limbs, whereas the generally steeply inclined foliations are measured along the other limb of F_2 folds. Occasionally observed steep inclination of the composite foliation (S_2) is probably caused by rotation during a later brittle deformation rather than representing a feature intrinsic to the D_2 style of deformation in the area. Axes b_1 of centimetre-scale rootless fold hinges F_1 are commonly perpendicular or at a high angle to b_2 (Fig. 4b), although several exceptions were also noted.

The stretching lineation observed on the main foliation S_2, represented by preferential growth of biotite and

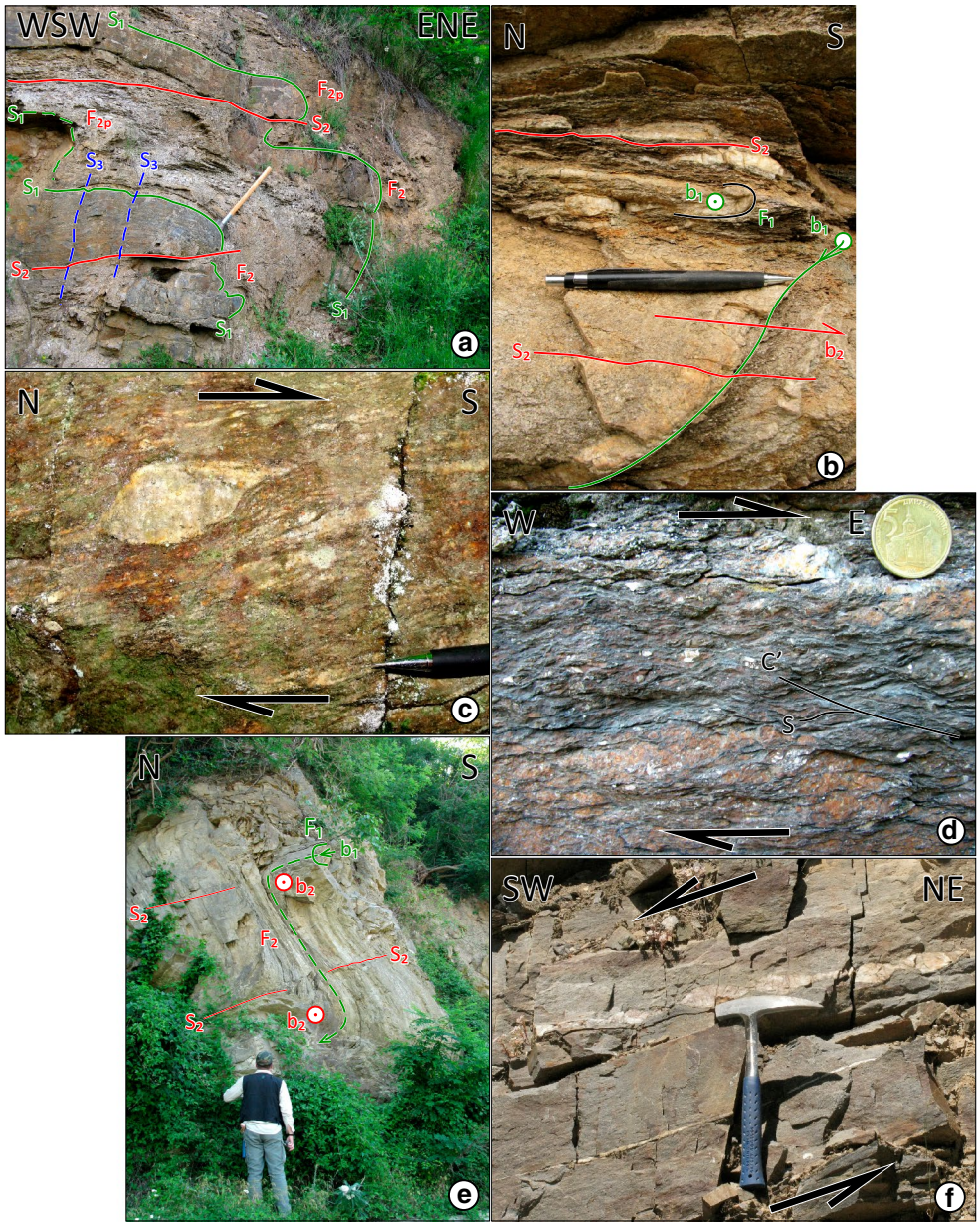

Fig. 5 **a** Folded alternation of gneiss, schists, and amphibolite in the western part of the Lower Complex (21°38′16.153″E, 42°45′8.295″N). Earlier foliation S_1 preserved in the competent amphibolites is folded into metre-scale isoclinal folds F_2 and parasitic folds F_{2p}. Minor transposition of limbs of F_2 folds along the axial-plane cleavage S_2 can also be observed. Late cleavage S_3 nearly perpendicular to the composite foliation S_1/S_2 is weakly developed. Length of hammer ca. 60 cm. **b** Micaschists in the western part of the Lower Complex (21°37′47.381″E, 42°45′8.195″N). Older isoclinal folds F_1 with fold axes b_1 perpendicular to the plane of image are refolded by isoclinal fold F_2 with fold axis parallel to the plane of image. Length of pencil 143 mm. **c** Polycrystalline sigmoid indicating top-to-the-south-west shear sense, west of the Vrvi Kobila shear zone (Fig. 3; 21°55′25.176″E, 42°49′19.199″N). Length of metal tip on a pencil 21 mm. **d** C' shear bands indicating top-to-the-east sense of shear in micaschists of the southern Lower Complex (21°53′27.018″E, 42°34′46.569″N). Coin diameter 24 mm. **e** Isoclinal folds F_1 from Vranjska Banja area refolded by asymmetric fold F_2 with axes b_2 perpendicular to the axis b_1 (22°4′38.741″E, 42°30′33.75″N). S_2 represents an axial-plane cleavage of folds F_2. **f** Layer-parallel train of asymmetric tapered boudins from Vranjska Banja area indicating top-to-the-south-west sense of shear (22°7′7.324″E, 42°29′57.556″N). Length of hammer 330 mm

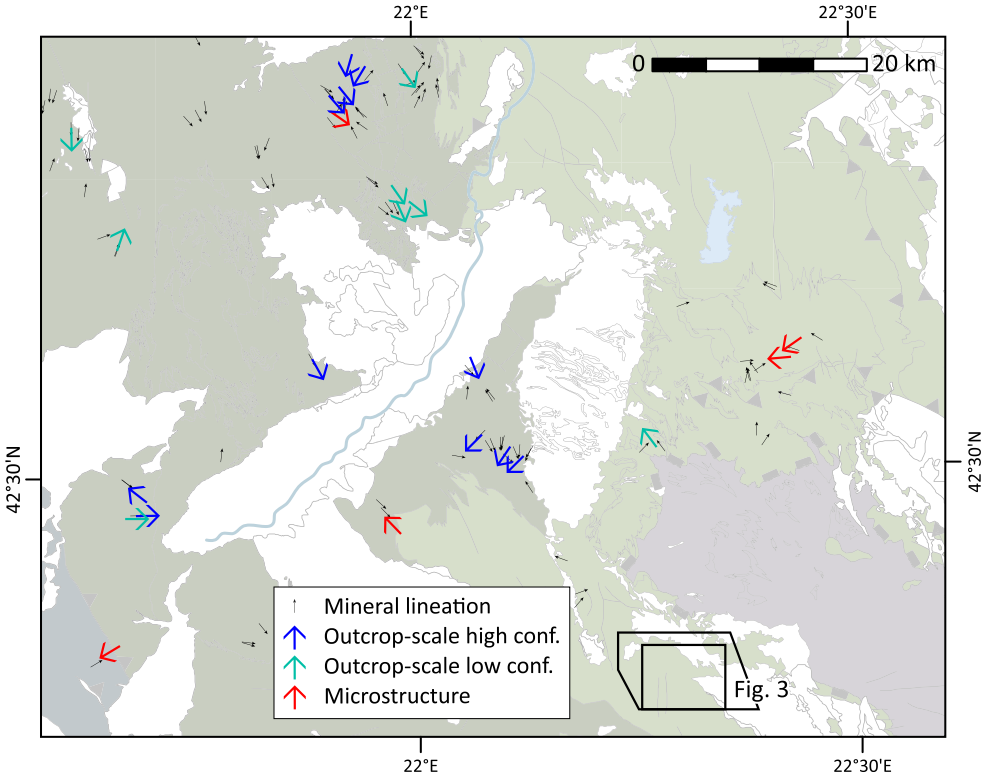

Fig. 6 Simplified tectonic map of the study area with *arrows* representing local directions of tectonic transport. See text for details

elongate ribbons of quartz, plunges gently in north-west–south-east direction (L_{min} in Fig. 4b). The fold axes b_2 of large recumbent folds F_2 generally exhibit a shallow to moderate plunge in virtually all directions, with a maximum towards the south to south-east (Fig. 4b). The apparent parallelism between stretching lineation and maximum of b_2 fold axes suggests that both structures are related to the same deformation stage (D_2). Later rotation of blocks in the brittle regime has caused further dispersion in the orientation of b_2 fold axes.

Crenulation cleavage S_3 intersects foliation S_2 at high angles and is generally subvertical to steep with apparently no preferred orientation (Fig. 4b). The orientation of b_3 axes is determined by calculating the intersection of foliation S_2 folded into large open folds in outcrop scale, or by scarce intersection lineation between S_2 and crenulation cleavage S_3. These axes are generally plunging in the south-western quadrant (Fig. 4b).

Kinematic indicators such as shear bands, polycrystalline sigmoids, and asymmetric clasts on outcrops, as well as biotite fish in thin sections, were observed in the *XZ* plane and indicate generally top-to-the-south to south-east sense of shear. Additionally, a number of σ-type mantled clasts and sigmoids in the same area show top-to-the-south-west sense of shear (Fig. 5c).

Low-grade retrogression of amphibolite-grade assemblage in this area is suggested by evidence of dynamic recrystallization of quartz by bulging (BLG) and late muscovite and sericite growth at the boundaries of feldspar grains.

Southern part of the Lower Complex

Penetrative foliation S_2 in the area surrounding the Bujanovac magmatic complex (Figs. 3, 4c) is generally dipping towards the east to south-east at moderate angles (Fig. 4c). It is commonly defined by biotite, muscovite, and flattened quartz–feldspar aggregates. Variation in orientation of S_2 is observed, but no apparent structural pattern could be established (Fig. 4c). The subhorizontal to shallow fold axes b_2 of tight to isoclinal folds F_2 are plunging towards the south-west and the north-east (Fig. 4c). Subvertical older foliation S_1 was observed only in the broad planar hinges of decametre-scale recumbent F_2 folds (Fig. 4c). Fold axes b_1 of small-scale rootless fold hinges F_1 are usually perpendicular to b_2 (Fig. 4c), with the exception of a single locality where the observed b_1 and b_2 are subparallel. Rarely observed stretching lineation defined by biotite and elongated quartz–feldspar aggregates is generally shallow to moderately plunging towards the south-east (Fig. 4c).

Cleavage S_3 related to large-scale open folds F_3 was observed at several locations, whereas north–south-directed subhorizontal plunge of fold axes b_3 was inferred from intersection lineation or calculated from the orientations of the limbs of gently folded S_2 (Fig. 4c).

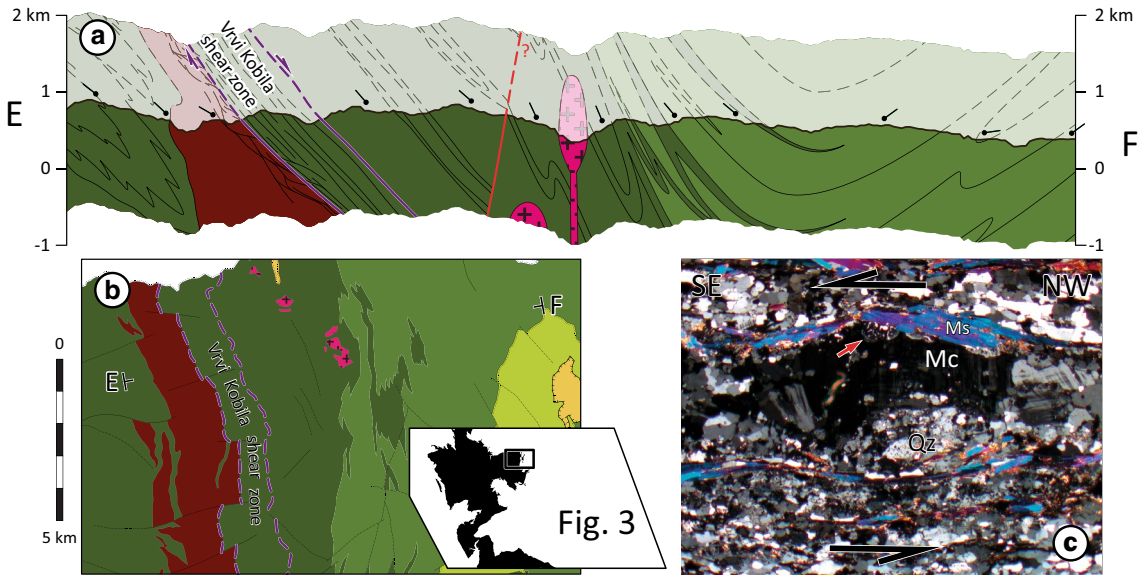

Fig. 7 **a** Cross-section EF through the Vrvi Kobila area. **b** Detail of the map in Fig. 2 with a trace of the cross-section EF. Location of the map relative to Fig. 3 and the Lower Complex (*black silhouette*) is indicated by a *black rectangle* in the *inset*. **c** Thin section of a mylonite within the Vrvi Kobila shear zone (SM01; 21°59′15.981″E, 42°42′27.645″N). *Red arrow points* to an asymmetric myrmekite. Large *black half-arrows* indicate sense of shear. Crossed nicols. Width of image 5.9 mm

C' shear bands observed in gneiss north of Vranje show top-to-the-south-east direction of tectonic transport (Figs. 5d, 6). C' shear bands, δ-type mantled clasts, and polycrystalline sigmoids observed in the western periphery of the Permo-Triassic pluton within the Bujanovac magmatic complex show top-to-the-E sense of shear, although a top-to-the-north-west shearing was also observed.

Vrvi Kobila area

Previous studies in the Vrvi Kobila area describe a 3-km-thick zone of intensive deformation, composed of phyllonites and mylonites (Vrvi Kobila fault zone, Petrović et al. 1973), along which the Vlasina Unit has been thrust onto the Lower Complex (Dimitrijević 1963; Vukanović et al. 1973; Krstić and Karamata 1992; Kräutner and Krstić 2002). Our studies in the area suggest the existence of a major ductile east-dipping shear zone with top-to-the-east to south-east sense of tectonic transport (Fig. 6). However, our observations also show that the hanging wall of the Vrvi Kobila shear zone is predominantly composed of two-mica gneiss and mica schists, which deviates from the typical lithological description of low-grade Vlasina Unit. Therefore, this shear zone does not separate the Lower Complex from the Vlasina Unit, as previously reported, and it is entirely developed within the former (Fig. 7). The presence of high-grade metamorphic rocks in the hanging wall was previously explained by the "granitisation effect" on the schists of Vlasina Unit in the hanging wall, exerted by the intrusion of Vlajna granite in the footwall (Petrović 1969; Vujanović et al. 1974). Our studies show that the emplacement of Vlajna granite (Antić et al. 2015b) predates the activity along the Vrvi Kobila shear zone, as a large part of this granite is deformed and transformed into coarse-grained gneiss that is observed within the zone and its hanging wall (Fig. 7a). Therefore, the extent of the Vlajna magmatic complex present on maps (Figs. 2, 3) and previous reports corresponds only to the weakly or undeformed part of the complex.

Foliation S_2 in the Vrvi Kobila area is moderately to steeply dipping towards the east (Fig. 4d). Variations in the orientation of S_2 are probably caused by the younger brittle deformation. The foliation S_2 is defined mostly by flattened quartz–feldspar aggregates and syn-deformational growth of muscovite and biotite. Several F_2 folds with axes b_2 generally parallel to the strike of the shear zone have been observed within low-strain domains in the area (Fig. 4d), as well as anastomosing shear zones in the Vlajna magmatic complex. Scarce subvertical to steep solution cleavage S_3 is striking north-east–south-west (Fig. 4d).

The stretching lineation represented by quartz–feldspar ribbons, muscovite, and biotite forms an array with two maximums, one towards the south-east and the other to the north-east (Fig. 4d). The lineations showing a maximum towards the south-east together with outcrop-scale sigmoids and asymmetrically stretched boudins which indicate top-to-the-south-east sense of shear were mainly observed along the Vrvi Kobila shear zone (Figs. 4d, 6).

This south-eastward shearing and the general south-east–north-west orientation of fold axes b_2 are considered to be related to deformation stage D_2. The lineations oriented differently than the south-eastern maximum could represent earlier structures not fully reworked during D_2 that were preserved away from the Vrvi Kobila shear zone (Fig. 6).

Vranjska Banja area

Metamorphic rocks of Vranjska Banja area, located between the Surdulica granodiorite and the Južna Morava River (Fig. 2), were traditionally attributed to Vlasina Unit, although they show evidence of higher metamorphic grade than the greenschist facies typical for the Vlasina Unit (Babović et al. 1977). Mineral assemblages in Vranjska Banja area showing the peak metamorphic conditions of 530–585 °C at 5.2–6.1 kbar (0.52–0.61 GPa, i.e. the boundary conditions between greenschist and amphibolite facies) are overprinting low-grade assemblages formed at 350–450 °C and 3.5 kbar (Vasković 1998; Vasković et al. 2003). As the division of central SMM into the Lower Complex and Vlasina Unit is generally based on the metamorphic grade, we designate the metamorphic rocks in Vranjska Banja area as a part of the Lower Complex (Figs. 2, 3).

Structural fabric of Vranjska Banja area was mostly examined along a Banjska river valley east of Vranje (Figs. 3, 8). Foliation S_2 in this area, predominantly defined by biotite, clinozoisite, and flattened quartz–feldspar aggregates, dips shallowly to moderately towards the south, with small populations dipping towards the south-east and south-west (Fig. 8d). Metre-scale asymmetric parasitic folds F_2 were observed in the limbs of presumed kilometre-scale recumbent folds (Figs. 5e, 8b), with shallowly plunging, east to south-east–west to south-west trending axes b_2. The earlier foliation S_1 was observed in the hinge areas of parasitic folds F_2, and it steeply dips towards the north-east and south-west (Fig. 8c). The rootless hinges of small folds F_1 are characterised by steep fold axes b_1 plunging towards south to south-east (Fig. 8b). Two axes b_3 of large folds F_3 were recognised based on the intersections of crenulation cleavage with foliation S_2 (Fig. 8b), and their shallow plunge towards south to south-west coincides with the π-axis of S_2 (Fig. 8d). The stretching lineation represented by preferential growth of biotite and muscovite observed on the main foliation S_2 plunges mainly towards the south-east and south-west with considerable scatter (L_{min} in Fig. 8a). The north-west–south-east strike of steep to subvertical spaced cleavage S_{SC} is nearly perpendicular to the trend of b_3 and therefore could not be related to D_3 but possibly represents much younger processes (Fig. 8e).

Two distinct zones of localised shear strain composed of highly deformed mylonitic to ultramylonitic rocks were

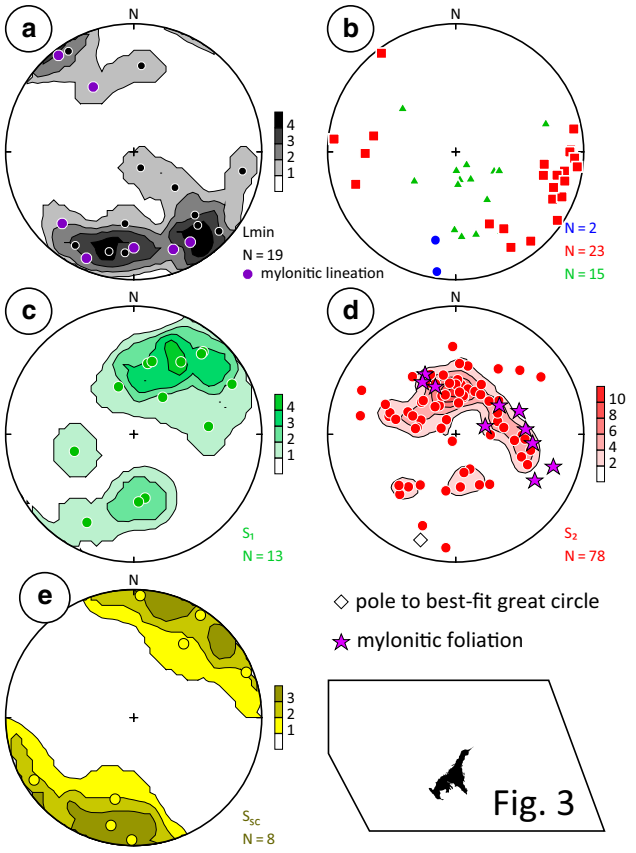

Fig. 8 Lower hemisphere equal-area plots of **a** mineral lineation, **b** fold axes, **c** poles to foliation related to D_1, **d** poles to foliation related to D_2, and **e** poles to spaced cleavage in Vranjska Banja area. See text for details. Symbol legend is given in Fig. 4. Relative scale and position in reference to Fig. 3 is given in the *inset*

observed in this area (Fig. 8d). Kinematic indicators such as foliation-parallel asymmetric drawn boudins (Fig. 5f; drawn- to shearband-boudin transition of Goscombe et al. 2004) and C' shear bands suggest top-to-the-south-west sense of shear (Fig. 6).

Vlasina Unit

Due to structural complexity encountered in the Vlasina Unit, its deformation pattern will be presented in three domains showing relative structural homogeneity (Fig. 9).

Southern part of Vlasina Unit

Penetrative foliation S_2 in the southern part of Vlasina Unit is subhorizontal to shallow dipping towards the south-east, with south-westward moderate to steep dip in a narrow area proximal to a belt of Eocene volcanic rocks south of Surdulica pluton (Figs. 3, 9a). The foliation S_2 often represents

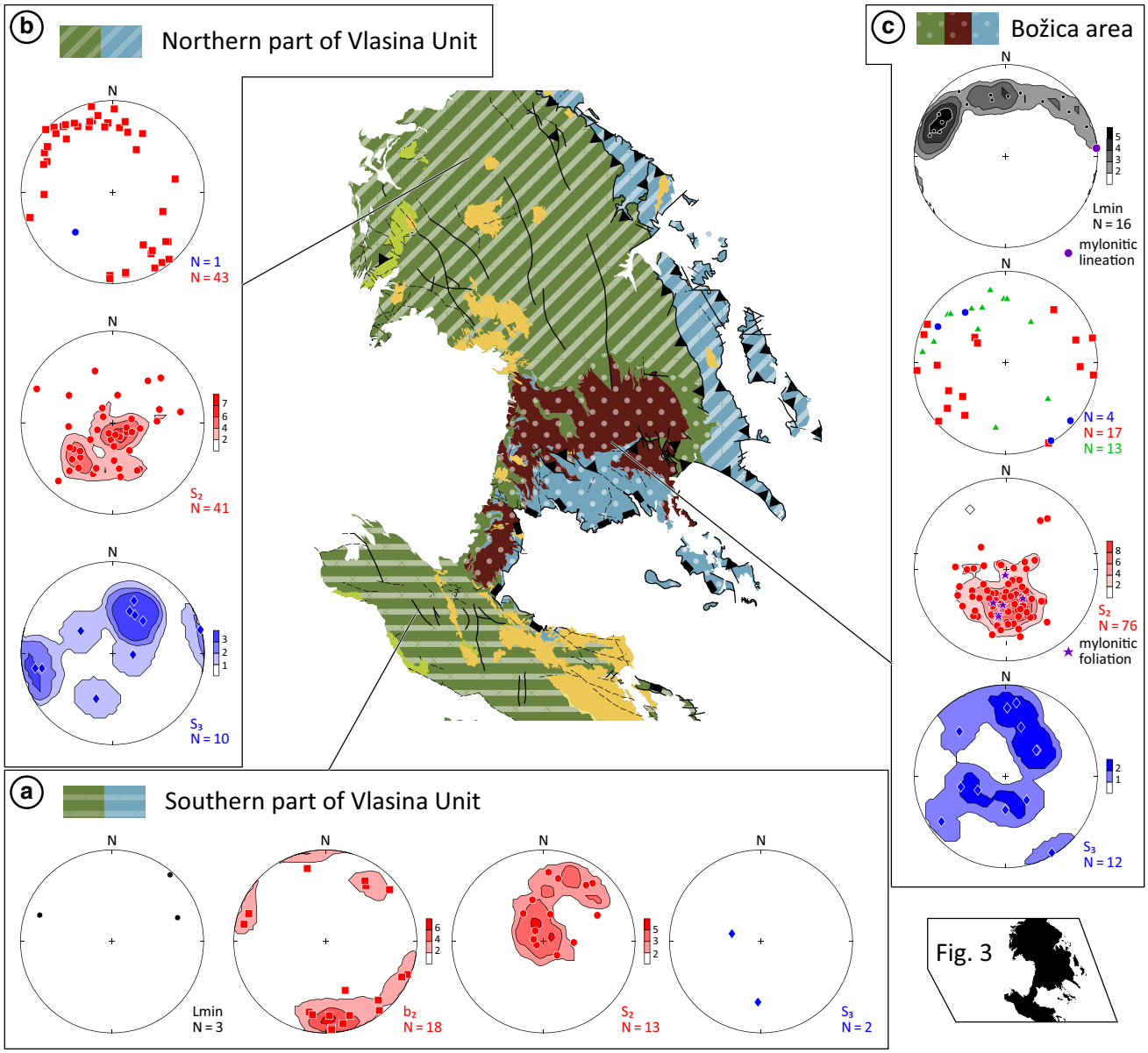

Fig. 9 Lower hemisphere equal-area plots of structural elements from the **a** southern part of Vlasina Unit, **b** northern part of Vlasina unit, and **c** Božica area. *Symbol legend* is given in Fig. 4. *Inset* shows the relative scale and position in Fig. 3

the axial-plane cleavage of tight to isoclinal recumbent folds F_2 (Fig. 10a). Due to their presumed kilometre-scale size, these folds F_2 are discernible only in hinge areas or by their decimetre- to metre-scale parasitic folds (Fig. 10a). Axes b_2 of these folds are plunging at low angles generally towards the south and south-east, and towards the north-east in the western periphery of this area (Figs. 3, 9a). Earlier folds F_1 are occasionally observed as isoclinally folded quartz–feldspar bands, refolded by F_2 (Fig. 10a). Due to small number of measurements, significance of mineral lineation and occurrences of late cleavage S_3 could not be critically evaluated in this area (Fig. 9a).

Northern part of Vlasina Unit

Ductile structures in the northern part of the Vlasina Unit were examined in the schists of the pre-Ordovician Vlasina as well in the post-Cambrian meta-sediments (Fig. 9b). Penetrative subhorizontal to shallow foliation S_2 is predominantly dipping towards the north-west with minor population dipping at moderate angles towards the north-east (Fig. 9b). The variation in the orientation of S_2 is assigned to subsequent brittle deformation, including Cretaceous east–north-eastward thrusting, especially prominent in the eastern part of this area. The foliation S_2 generally

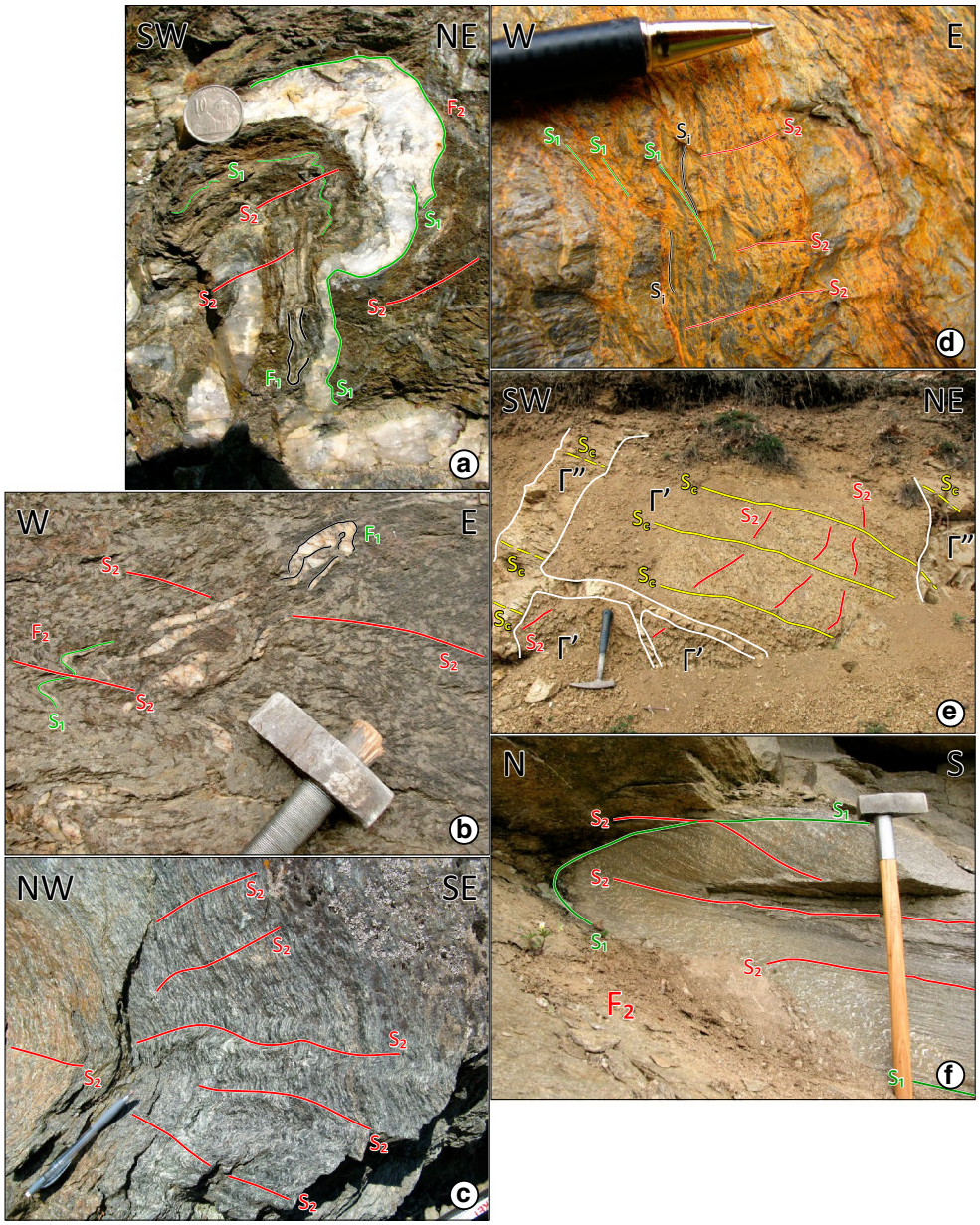

Fig. 10 **a** Isoclinal fold F_1 refolded by later isoclinal fold F_2 with axial-plane cleavage S_2 in chlorite–muscovite schists in the southern part of the Vlasina Unit (22°5′52.149″E, 42°22′5.121″N). Diameter of coin 26 mm. **b** Quartz–feldspar bands folded into isoclinal folds F_1 represented by rootless hinges in a matrix of chlorite–muscovite schists in the northern part of Vlasina Unit (22°4′57.756″E, 42°53′43.306″N). Size of the head of hammer 136 mm. **c** Fanning axial-plane cleavage S_2 in the chlorite schists in the northern part of Vlasina Unit (22°18′15.775″E, 42°48′21.52″N). Size of pen 152 mm. **d** Initial foliation S_i folded in centimetre-scale chevron folds F_1 preserved only as limbs due to strong reworking by the axial-plane cleavage S_1, with superimposed crenulation cleavage S_2 in upper Silurian to Lower Devonian argillites of the northern part of Vlasina Unit (22°32′33.657″E, 42°45′9.631″N). Size of metal tip of a pen 17 mm. **e** Spaced cleavage S_c is observed in the early Silurian coarse-grained Qz-monzonite (Γ') and Permo-Triassic fine-grained granites (Γ''), whereas the foliation S_2 can be seen only in the former (21°49′51.156″E, 42°21′30.213″N). Hammer length 330 mm. **f** Refraction of S_2 in the folded granodiorite in the western part of the Lower Complex (21°37′48.583″E, 42°45′9.15″N). Length of hammer ca. 60 cm

represents axial-plane cleavage of recumbent decimetre- to decametre-scale tight to isoclinal folds F_2 (Fig. 10b, c). Foliation S_2 is defined by muscovite and chlorite. Fold axes b_2 are predominantly subhorizontally to shallowly plunging in north to north-west–south to south-east direction (Fig. 9b). An initial foliation S_i is defined by quartz–feldspar bands that were isoclinally folded into centimetre-scale folds F_1 (Fig. 10b) and subsequently refolded into

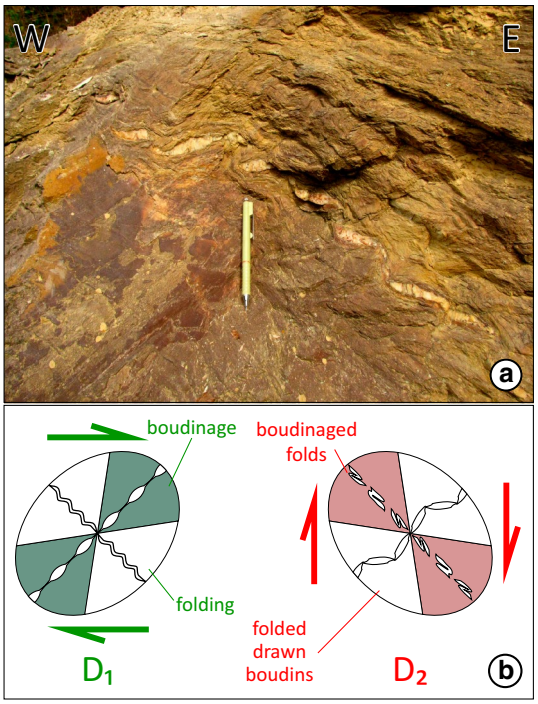

Fig. 11 **a** Folded train of drawn boudins within the Ordovician meta-argillites in the northern part of Vlasina Unit (22°25′47.903″E, 42°51′49.239″N). Size of pencil 13.5 mm. **b** Evolution of structures through deformation stages D_1 and D_2. *Shaded areas* of strain *ellipsoids* represent extensional quadrants, whereas *blank areas* represent compressional quadrants

large recumbent folds F_2. This initial foliation (S_i) is better observed in the thrust sheets composed of low- to very-low-grade Lower Palaeozoic meta-sediments (Fig. 3). In the upper Silurian to Lower Devonian argillites, the foliation S_i is defined by sericite-rich bands folded in centimetre-scale chevron folds F_1, of which only limbs have remained due to strong reworking by the axial-plane cleavage S_1, whereas the late S_2 represents a crenulation cleavage developed at a high angle to S_1 (Fig. 10d).

The difference in orientation of strain axes during the deformation stages D_1 and D_2 resulted in the formation of folded drawn boudin trains in Ordovician meta-argillites (Fig. 11). The boudin trains were initially formed in the extensional domain of D_1 strain ellipsoid and were subsequently folded by simple shearing during D_2 (Fig. 11b).

Spaced and crenulation cleavage S_3 was distinguished only where it intersects composite foliation at high angles in medium- to low-grade rocks, generally in areas close to Južna Morava River (Fig. 3). Maximum of S_3 is dipping towards the north-east at a moderate angle, but a significant population of subvertical cleavage striking north to north-east–south to south-west is also observed (Fig. 9b). A single axis b_3 moderately plunging towards the south-west of a large open fold F_3 was measured in an area away from the thrust front (Fig. 9b).

Božica area

Božica area comprises the Božica magmatic complex and the post-Cambrian meta-sedimentary succession (Lisina series of Dimitrijević 1963; Babović et al. 1977), south of the magmatic complex (Figs. 3, 9c). In this area, foliation S_2 is generally dipping at moderate to low angles towards the north (Fig. 9). Fold axes b_2 of decimetre-scale asymmetric parasitic folds F_2 are trending east to south-east–west to north-west (Figs. 9c, 12a). Foliation S_2 represents an axial-plane cleavage of folds F_2 (Fig. 12a). Earlier centimetre-scale isoclinal folds F_1 are preserved as rootless fold hinges, refolded by F_2 at various intersection angles (Figs. 9c, 12a).

Late crenulation (Fig. 12b) or spaced cleavage S_3 is usually distinguished by high intersection angles with S_2, and it is moderately to steeply dipping with no preferential direction (Fig. 9c). Subhorizontal to shallow fold axes b_3 trending north to north-west–south to south-east are inferred from intersection lineation of S_3 on S_2 and crenulation lineation (Fig. 9c). The mineral lineation statistically forms a girdle with approximate orientation 000/30 having a single maximum at 304/20 (Dip direction/Dip angle; Fig. 9c). Although neatly aligned in the spherical projection, these lineations are anisotropically distributed throughout the Božica area.

The presence of mylonite, ultramylonite, and discrete anastomosing shear zones developed in the southern part of Božica magmatic complex indicates that these rocks have experienced considerable amount of shear strain (Fig. 12c). Foliation is defined by syn-deformational muscovite, biotite, and clinozoisite. Kinematic indicators such as δ- and σ-type mantled clasts of feldspar (Fig. 12d) indicate top-to-the-west to south-west sense of shear (Fig. 6).

Eastern Veles series

Structural data from the EVS were collected only along a single transect across the contact with the Lower Complex, north of Preševo (Figs. 2, 3). Although the contact itself could not be directly observed, it was established that the penetrative foliation in the EVS is steeply dipping towards east to north-east (Fig. 13a) being parallel to the orientation of S_2 in the Lower Complex near the contact (Fig. 4). Structural concordance between these penetrative fabrics suggests a ductile character of the contact. The foliation in gneisses of the EVS is defined by flattened quartz–feldspar aggregates, biotite, and muscovite. Asymmetric K-feldspar grains (sheared boudin trains, sigmoids, and δ-like clasts) in late Cambrian leucocratic orthogneiss (Antić et al. 2015b)

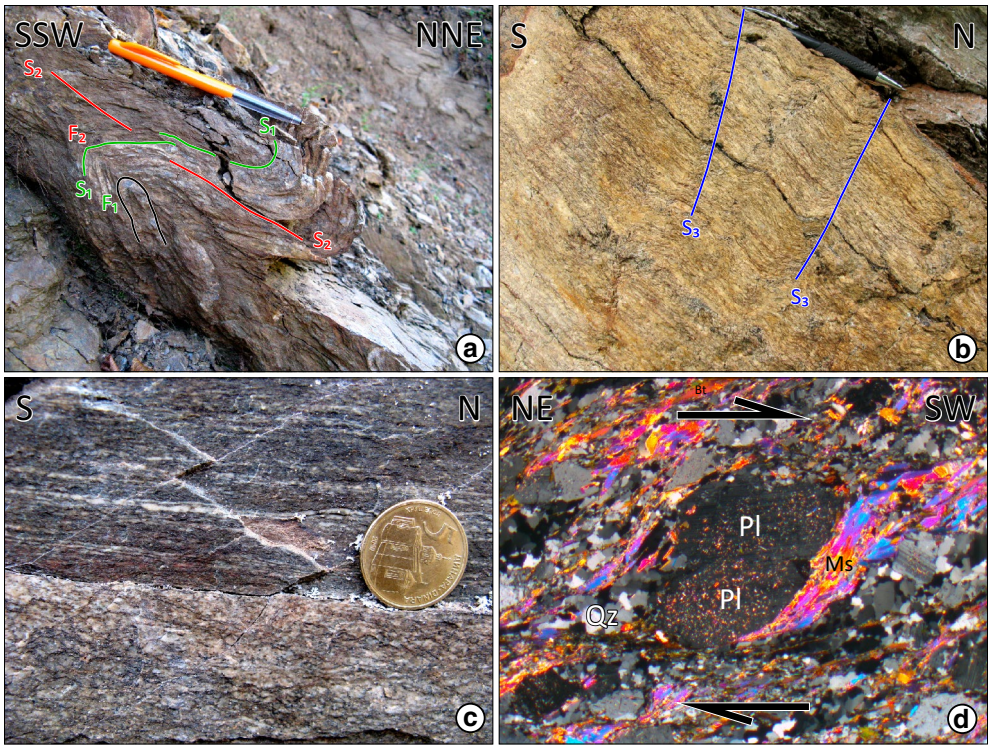

Fig. 12 Structural features in the Božica area: **a** Rootless hinges of folds F_1 in the hinge of isoclinal fold F_2 in Ordovician sericite–chlorite schists (22°23′8.132″E, 42°33′6.694″N). Minor transposition of S_1 along axial-plane cleavage S_2 can also be observed. Size of pen 145 mm. **b** Crenulation cleavage S_3 in the mylonites formed in the Božica magmatic complex (22°23′40.552″E, 42°35′28.461″N). Length of pencil 143 mm. **c** Ultramylonites within the Božica magmatic complex (22°23′40.552″E, 42°35′28.461″N). Diameter of the coin 24 mm. **d** A σ-type K-feldspar mantled porphyroblasts indicating top-to-the-south-west sense of shear (SM272-1; 22°24′50.956″E, 42°35′42.182″N). Crossed nicols. Width of image 5.9 mm

indicate top-to-the-south-west sense of shear (Figs. 6, 13b). Replacement of K-feldspar by muscovite and sericite is widespread (Fig. 13b). Quartz grains show sweeping undulose extinction and deformation lamellae as well as evidence of dynamic recrystallisation predominantly by grain boundary migration (GBM) with less prominent evidence of subgrain rotation (SGR; Fig. 13b).

Permo-Triassic Bujanovac pluton

The Bujanovac magmatic complex encompasses two distinct generations of igneous rocks: (1) a coarse-grained quartz–monzonite emplaced in early Silurian intruded by (2) a fine-grained granite in late Permian to Early Triassic (Antić et al. 2015b). The early Silurian monzonite is strongly deformed and transformed into gneiss with a penetrative regional foliation S_2. Field observations revealed a weakly developed cleavage S_C in both the younger and the older magmatic rocks (Fig. 10e). Occasionally, this late cleavage S_C in the old quartz–monzonite intersects the older foliation S_2 at low angles, resulting in a structure similar to pencil cleavage (Fig. 10e). Late cleavage S_C predominantly dips at moderate angles towards the north-east (Fig. 13c). Macroscopic S–C fabric observed in central parts of the younger fine-grained granite shows a general top-to-the-north shear direction. Additionally, a number of anastomosing shear zones separating low-strain domains were observed in the younger granite.

$^{40}Ar/^{39}Ar$ thermochronology

An overview of the $^{40}Ar/^{39}Ar$ thermochronology method is given in online Appendix A together with a detailed description of the analysed material and complete $^{40}Ar/^{39}Ar$ data. A brief overview of critical sample information is given in Table 1, while relevant $^{40}Ar/^{39}Ar$ date spectra, K/Ca diagrams, and isotope correlation plots are shown in Fig. 14. Additionally, the $^{40}Ar/^{39}Ar$ dates are presented in Fig. 2 along with previously published K/Ar, Rb/Sr, and $^{40}Ar/^{39}Ar$ dates. Plateau date is defined by at least three contiguous heating steps with indistinguishable dates spanning more than 50 % of the ^{39}Ar released (Dalrymple and Lanphere 1974). The $^{40}Ar/^{39}Ar$ date is considered robust only if the plateau age overlaps with the inverse isochron date. When these conditions are not met, the weighted mean date is

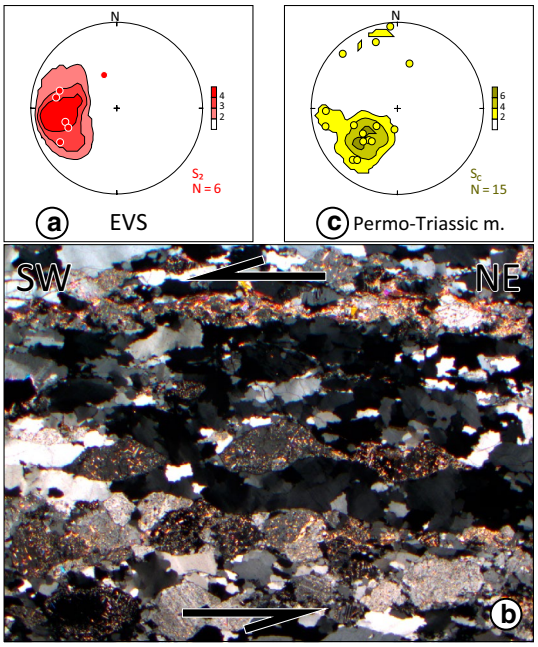

Fig. 13 Lower hemisphere equal-area plot of **a** the measured foliation S_2 in the EVS. **b** Asymmetric K-feldspar *grains* indicating top-to-the-south-west sense of shear in leucocratic orthogneiss in the EVS (SM315; 21°38′37.896″E, 42°20′43.603″N). Crossed nicols. Width of the image 5.9 mm. **c** Lower hemisphere equal-area plot of spaced cleavage S_c in Permo-Triassic magmatic rocks (i.e. fine-grained Bujanovac granite)

used, which is defined by at least three contiguous heating steps that yield dates that differ by less than 5 %, and span at least 50 % of ^{39}Ar released. Mineral names are abbreviated according to Whitney and Evans (2010).

Newly formed muscovite (i.e. without inherited domains) that defines a mylonitic foliation within the Vrvi Kobila shear zone yielded an early Carboniferous plateau date (351 ± 1 Ma; SM01; Table 1; Figs. 2, 7c, 14). Thermal history of the Vlasina Unit was examined by analysing undeformed muscovite from chlorite schists, which showed a lower Permian plateau date (284 ± 1 Ma; SM05; Table 1; Figs. 2, 14). An aliquot of syn-tectonic biotite from a mylonite formed under higher-greenschist facies conditions, sampled within a shear zone with a top-to-the-west sense of shear formed in the Božica magmatic complex, yielded a Middle Triassic plateau date (246 ± 1 Ma; SM499-1; Table 1; Figs. 2, 14). Thermal evolution of a Lower Complex gneiss that experienced retrogression was investigated by analysis of biotite grains that are forming the foliation in these rocks and have not been affected by retrogression. These biotites showed Lower Jurassic plateau date (195 ± 1 Ma; SM248-1; Table 1; Figs. 2, 14). Two remaining biotite samples (SM437-1 and SM250-2) and a hornblende concentrate (SM250-1) yielded more ambiguous results reported only as weighted mean dates (338 ± 2, 182 ± 6, and 290 ± 8 Ma, respectively). These results are interpreted only by consideration of additional geological observations (Table 1; Figs. 2, 14).

Discussion

The results of structural analysis and ^{40}Ar/^{39}Ar thermochronology revealed a sequence of major tectonothermal events that affected the central SMM. The individual stages of deformational and thermal evolution are discussed below in chronological order.

Variscan Orogeny

First deformation stage D_1

Evidence of deformation stage D_1 is generally scarce, as the resulting structures have been strongly overprinted during the subsequent deformation stage D_2. Structures formed during D_1 were documented in both the Lower Complex (e.g. Fig. 5b) and the Vlasina Unit (e.g. Figs. 5f, 12a). The most common structural elements preserved from this stage are centimetre-scale rootless hinges of folds F_1 in the microlithons bound by foliation S_2, with fold axes b_1 usually at high angles to axes b_2 of younger folds F_2. Rarely, refolded decimetre-scale folds F_1 could be observed in the hinge areas of larger folds F_2 (Fig. 5e). As an exception, structures related to D_1 were better preserved in the low-grade meta-sediments of the post-Cambrian Vlasina, located in the Cretaceous thrust sheets in the north-eastern part of the study area (Fig. 3). These structures include folds F_1 and drawn boudin trains showing only minor deformational overprint related to D_2 (Figs. 10d, 11a, respectively).

The strong overprint during D_2 in most of the study area and the subsequent brittle deformation do not allow reconstruction of either the general orientation of main stress axes, or the direction of tectonic transport during D_1. Likewise, none of the observed stretching lineations could be unequivocally attributed to D_1. At locations where the stretching lineations were considered as related to D_1 due to their misalignment to the perceived general trend (e.g. Vrvi Kobila area), their original orientation was not preserved due to reworking during D_2 as shown by the complete transposition of S_1. However, the intersection angles between fold axes b_1 and b_2, ranging within 90° (Figs. 4, 8b, 9), could be interpreted as a consequence of the initial orientation of b_1, or exclusively a result of varying intensity of the later deformational overprint(s).

Based on the similarities in structural style, the deformation stage D_1 corresponds to the "phase I" from the detailed structural study of the Vlasina Unit by Petrović (1969). The

Table 1 Overview of the results of $^{40}Ar/^{39}Ar$ thermochronology

Sample name	Locality	Rock type	Tectonic unit	Sampling location (DMS)		Elevation (m asl)	Mineral phase	$^{40}Ar/^{39}Ar$ date (Ma)	$\pm 2\sigma$ (Ma)	$^{39}Ar_k$[a] (%)	Inverse isochron date (Ma)	$\pm 2\sigma$ (Ma)	MSWD[b]
				Longitude	Latitude								
SM01	Kukavica	Mylonite	Lower Complex	22°0′50.825″E	42°41′39.368″N	738	Ms	351 (P)	1	59.87	352	2	n/a
SM05	Predejane	Chl-schist	Vlasina Unit	22°5′9.39″E	42°48′45.797″N	309	Ms	284 (P)	1	46	285	1	0.49
SM248-1	Vlajna	Bt-gneiss	Lower Complex	21°56′45.673″E	42°48′12.532″N	599	Bt	195 (P)	1	58.35	195	3	2.58
SM250-1	Golemo Selo	Amphibolite	Lower Complex	21°50′38.126″E	42°43′54.05″N	485	Hbl	290 (W)	8	54.69	234	28	36.58
SM250-2	Golemo Selo	Bt-gneiss	Lower Complex	21°50′38.126″E	42°43′54.05″N	485	Bt	179 (W)	1	96.81	185	3	9.56
SM437-1	Vranjska Banja	Mylonite	Lower Complex	21°53′58.876″E	42°27′45.765″N	483	Bt	338 (W)	2	78.57	345	12	2.81
SM499-1	Božica	Mylonite	Vlasina Unit	22°24′2.255″E	42°35′38.648″N	1112	Bt	246 (P)	1	56.48	247	1	0.58

Weighted mean dates (W) are tentative, and their interpretation requires caution. See text for details

Mass discrimination factor = 0.983 ± 0.051

Mineral names abbreviated according to Whitney and Evans (2010): *Ms* muscovite, *Bt* biotite, *Hbl* hornblende, *EVS* Eastern Veles series, *P* plateau, i.e. >3 contiguous heating steps that span >50 % ^{39}Ar released (the date is the weighted mean date of the plateau), *W* weighted mean date of >3 contiguous heating steps that yield distinguishable dates that differ by less than 5 %, and span >50 % ^{39}Ar released

[a] Percentage of ^{39}Ar released during steps used in data calculation

[b] Mean square of weighted deviates of the inverse isochron linear regression

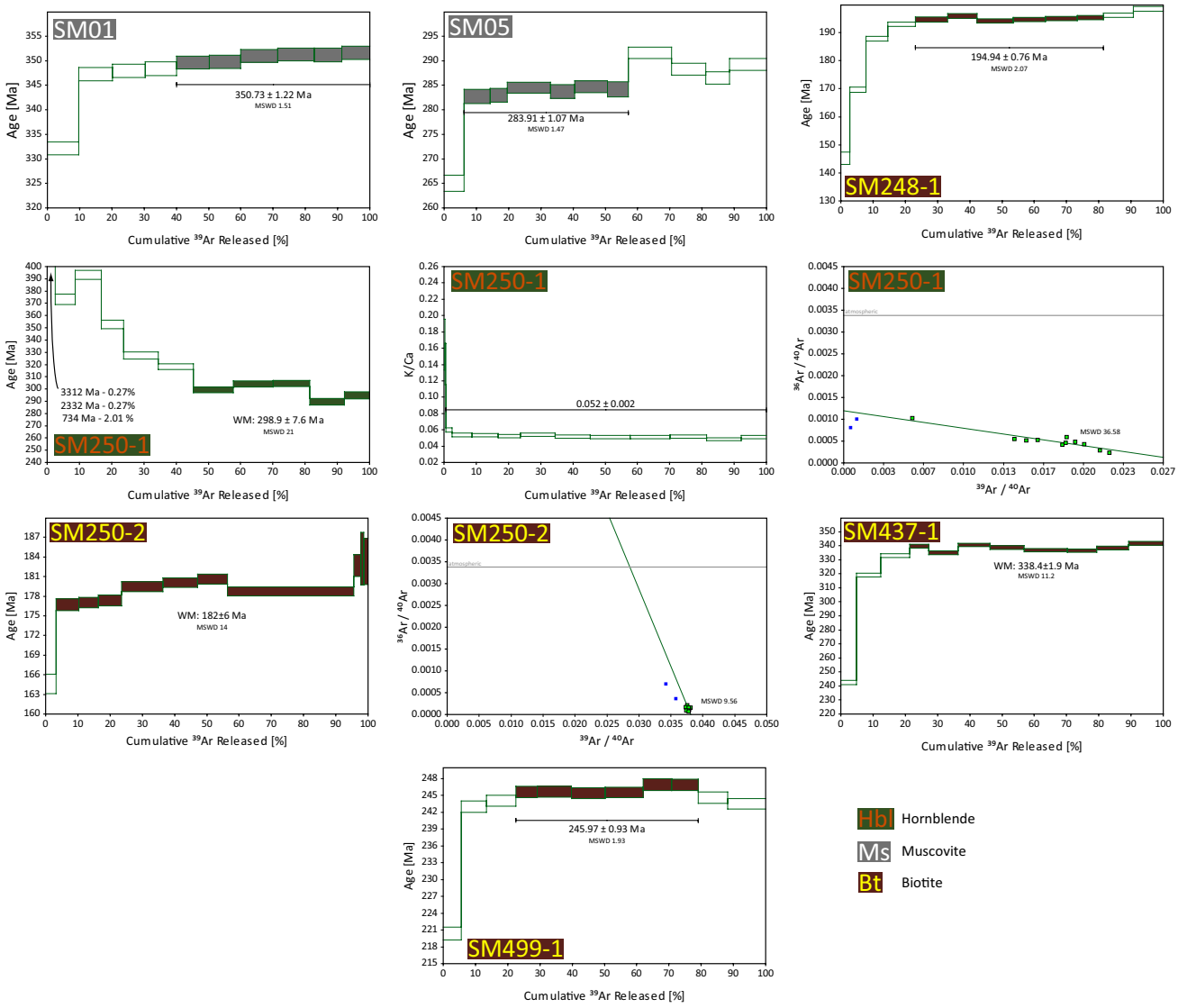

Fig. 14 Relevant $^{40}Ar/^{39}Ar$ date spectra, K/Ca yield diagrams, and isotope correlation plots for samples from the central SMM. All uncertainties are $\pm 2\sigma$. Plateau dates are defined according to Dalrymple and Lanphere (1974). *WM* weighted mean date. See online Appendix A for further details

youngest rocks containing the effects of D_1 are the upper Silurian to Lower Devonian meta-sediments (Marinova et al. 2010) in the thrust sheets of post-Cambrian Vlasina (Fig. 10d), thus constraining a maximum age of D_1 to the lower Emsian (ca. 408 ± 3 Ma; Cohen et al. 2013). Minimum age constraints on D_1 could not be clearly defined, but it certainly predates the onset of the deformation stage D_2, which is discussed below.

Second deformation stage D_2

Penetrative foliation S_2 shows predominantly subhorizontal to shallow dip since it formed as an axial-plane cleavage to the kilometre-scale recumbent folds F_2 (Figs. 4, 8b, 9, 13a). These large folds could be detected only by the asymmetric parasitic folds at decimetre- to metre-scales (e.g. Figs. 5e, 8b, 10a, c). Foliation S_2 in the hinge areas of these folds is observed as axial-plane cleavage (Fig. 10f), whereas in the limbs, the older foliation(s) are completely transposed.

Although its orientation generally varies in individual domains presented above, the fold axes b_2 of recumbent isoclinal folds F_2 most often show similar orientation to that of the stretching lineation, which is assumed to be formed during D_2 (Fig. 4a, b). This parallelism is commonly reported in domains deformed by recumbent folds (Bastida et al. 2014 and references therein), and it could result from a progressive deformation during D_2 (sensu

Tobisch and Paterson 1988), implying a relatively constant orientation of the regional stress field in a geologically short period of time producing various sets of structures with similar orientation, sense of movement, style, and prevailing metamorphic conditions. It is possible that during the early stages of D_2, the isoclinal folds F_2 were initiated, whereas these folds were amplified into recumbent and less cylindrical forms in the later stage of the same deformation stage. A progressive non-coaxial deformation would cause an amplification of folds while increasing the curvature of hinge lines leading to the reorientation of fold axes b_2, and eventually to transposition of older structures along S_2 during the late D_2. The suggested partial reorientation of fold axes b_2 could explain the observed dispersion in their orientation (e.g. Figs. 4, 8b, 9). Alternatively, the parallelism of linear elements (i.e. fold axes b_2 and stretching lineation) to the direction of tectonic transport could be explained by the laterally constricted thrusting (Fossen 1993; Passchier et al. 1997; Fernández et al. 2007). In this case, the western part of the Lower Complex seems to be affected the most based on the uniformity of linear structures it displays (Fig. 4a). This might be a consequence of the lowermost position in the crust it held during the Variscan orogeny and thus the least rheological competence. The effects of this mode of deformation (i.e. parallelism between the stretching lineation and the fold axes b_2) are less evident in the remaining areas of the central SMM, which were presumably at relatively shallower depths during D_2. Additionally, local variations in geometry of all structural elements formed during D_2 were probably disturbed further during the subsequent events involving magmatic intrusions and block rotations in the brittle regime.

The majority of the observed kinematic indicators in central SMM suggest south-eastward direction of tectonic transport (Fig. 6). This transport direction is most probably related to the last high-strain event in the area—D_2, together with the corresponding mineral lineation trending north-west–south-east (Figs. 4, 8a, 9c). Several exceptions are observed in the western domain of the Lower Complex and the Vranjska Banja area (Figs. 4a, 8a). In the western part of the Lower Complex (i.e. west of Tupale fault; Fig. 4a), stretching lineation L_{min} and fold axes b_2 trend generally north–south. The misalignment of these structures with the prevailing north-west–south-east trend could be caused by a local difference in D_2 strain field or represents mineral lineation from an early D_2 that were incompletely rotated during progressive deformation. Similar south to south-westward plunge of stretching lineation together with south-westward sense of shear was observed in the Vranjska Banja area. Furthermore, the observed scatter in the orientation of stretching lineation and shear sense indicators could be a result of block rotation in the brittle regime during the Alpine orogeny, which had considerably reshaped this area (Antić et al. 2015a). Additionally, the rheological contrast between adjacent domains could have caused the observed opposite senses of shear (Burg 1987). The stretching lineations and shear sense indicators were rarely observed in the Vlasina Unit, except for the deformation in Božica area, which will be discussed below.

The metamorphic grade and strain intensity within the central SMM are observed to decrease eastwards (in present coordinates, i.e. from the Lower Complex to the metasediments in the post-Cambrian Vlasina). A probable cause for this trend could be the structural level of these units within the Variscan orogen. The amphibolite-grade Lower Complex was in a mid-crustal position, whereas the pre-Ordovician Vlasina with mineral assemblages indicating greenschist facies peak conditions was located within the upper crust, below the anchimetamorphosed rocks of the post-Cambrian Vlasina. Vranjska Banja and Božica areas with transitional metamorphic grade between amphibolite and greenschists facies probably held intermediate crustal positions. Abrupt changes in metamorphic grade observed across brittle thrusts in the eastern part of the study area could be explained by telescoping during the Cretaceous compression.

The general south-eastward tectonic transport during D_2 cannot explain the increase in the metamorphic grade from east to west observed in the studied area. This metamorphic pattern must be related to a general westward thrusting and thickening of the crust. Therefore, we suggest that the westward sense of tectonic transport was most probably related to stage D_1, when the peak metamorphic conditions were attained in the central SMM.

The minimum age of deformation stage D_2 is constrained by the undeformed Slatinska Reka granite, which intruded the Lower Complex gneisses in the Vrvi Kobila region at 328 ± 5 Ma (U–Pb zircon age; Antić et al. 2015b). At the contact with these granites, the hinge of F_2 open fold with well-developed axial-plane cleavage S_2 was observed together with rootless hinge of fold F_1 generated during the earlier deformation stage D_1 (Fig. 15). These observations clearly show that the granite intrusion postdates both D_1 and D_2 deformation stages.

Based on the style of deformation, structures generated during progressive deformation of D_2 are comparable to those of "phases II and III" previously established as synmetamorphic folding stages in the Vlasina Unit (Petrović 1969).

Indirect constraints on the age of both deformation stages D_1 and D_2 presented above suggest that they have taken place during the Variscan orogeny (i.e. between 408 and 328 Ma, lower age limit is discussed further below). At this time, the central SMM was involved in a series of tectonic events related to amalgamation of eastern and western parts of the Galatian super-terrane and its final collision

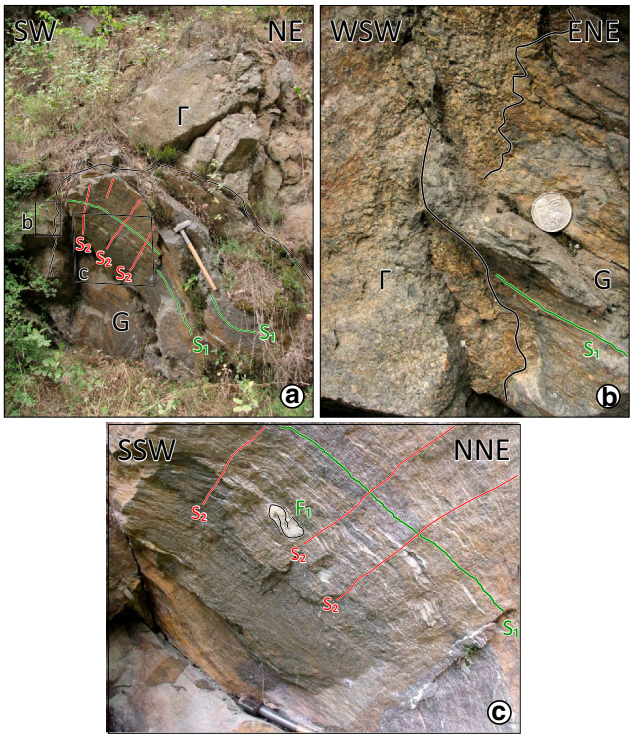

Fig. 15 **a** Intrusive contact of Slatinska Reka granite (Γ) and Lower Complex gneiss (G) in the Slatinska Reka Valley (22°1′30.716″E, 42°50′53.365″N). Trace of the contact plane is indicated by *black line*. S_1 foliation formed during D_1 and folded into isoclinal folds F_2; S_2 axial-plane cleavage related to folds F_2 during D_2. Length of hammer ca. 60 cm. **b** Detail from **a**. Diameter of the coin 26 mm. **c** Detail from **a** showing the quartzitic rootless hinge of fold F_1 and axial-plane cleavage S_2 of fold F_2. Hammer head length 134 mm

with Laurussia (Stampfli et al. 2013; Antić et al. 2015b). Variscan age of the peak metamorphism and high-strain deformation has been reported for a number of crystalline units in the Carpatho-Balkanide orogen (Dimitrijević 1958; Dallmeyer et al. 1998; Ilic et al. 2005; Carrigan et al. 2005; Karamata 2006). North–south-oriented compression (in present orientation) related to the Variscan orogeny was previously reported for the crystalline basement of the Getic tectonic zone in Romania (Plissart et al. 2012). Farther east in the Central Stara Planina Unit of the Balkan belt, Gerdjikov et al. (2010a, b) reported an Early Carboniferous (336–315 Ma) km-scale transpressional ductile shear zone trending east–west that juxtaposes higher-grade over lower-grade Variscan metamorphic rocks. The remnants of the Variscan orogen in the Balkan belt represent a direct prolongation of the Variscan metamorphic rocks from the Getic zone and the SMM that have experienced clockwise rotation and dextral strike-slip tectonics during the Alpine orogeny (e.g. Csontos and Vörös 2004; Fügenschuh and Schmid 2005).

The evidence of pre-Variscan deformation and HP metamorphism proposed previously (Dimitrijević 1959; Petrović 1969; Milovanović 1989; Balogh et al. 1994; Karamata and Krstić 1996; Zagorchev and Milovanović 2006) was not observed during this study.

High occurrence of mylonites observed in the Vrvi Kobila area together with anastomosing shear zones in the competent magmatic rocks of the Vlajna magmatic complex (Figs. 2, 7) constitutes an important shear zone characterised by south-eastward direction of tectonic transport. Evidence of dynamically recrystallised quartz by GBM and SGR (Stipp et al. 2002), along with asymmetric myrmekite (Fig. 7c; Simpson and Wintsch 1989), indicates that this shear zone was active during high-grade conditions. Folding within this area was observed only in isolated low-strain zones and in the periphery of the shear zone (Figs. 7a, 15). Observations made during this study show that this shear zone does not separate the Lower Complex from the Vlasina Unit as previously reported, but it is entirely formed within the former (discussed above). Discrete contact between these two units was not directly observed in the study area. However, the proximity of amphibolite facies gneisses of Lower Complex and greenschist facies rocks of Vlasina Unit in the hanging wall of the Vrvi Kobila shear zone, and relative structural concordance of foliation S_2 in both rock types suggest that some telescoping must have occurred prior to the end of stage D_2 (Fig. 7a, b). It must be noted that apart from difference in metamorphic grade, the metamorphic rocks of Lower Complex and Vlasina Unit also had different protoliths. Therefore, the speculative structure that had telescoped the metamorphic sequence, also had juxtaposed two contrasting protolith lithologies.

An early Carboniferous $^{40}Ar/^{39}Ar$ plateau date of muscovite from the Vrvi Kobila area (SM01: 351 ± 1 Ma) is interpreted as the minimum age of activity along this shear zone which most probably took place during deformation stage D_2 (Figs. 2, 14, 16). A similar Rb–Sr date of 349 Ma was reported for muscovite from the leucocratic vein in the Lower Complex, north of the research area (i.e. north of Lece volcanic complex in Fig. 2; Deleon 1969). Nevertheless, the possibility that the Vrvi Kobila shear zone is related to a post-D_2 late orogenic extension cannot be entirely ruled out. This shear zone was previously considered as a continuation of the Gabrov Dol detachment in Bulgaria, which was reported as a Cretaceous extensional boundary between the Bulgarian equivalent of Lower Complex (i.e. Ograzhden unit) and Vlasina Unit (i.e. low-grade ophiolitic rocks of Struma unit; Zagorchev 1984; Bonev et al. 1995; Ricou et al. 1998). Later, the Cretaceous age of this complex structure was rejected, and it was related to the Variscan orogeny (Kounov et al. 2010; Gerdjikov et al. 2013; Antić et al. 2015a, b). However, Vrvi Kobila and Gabrov Dol shear zones do not share the same tectonic position nor the same metamorphic grade of the

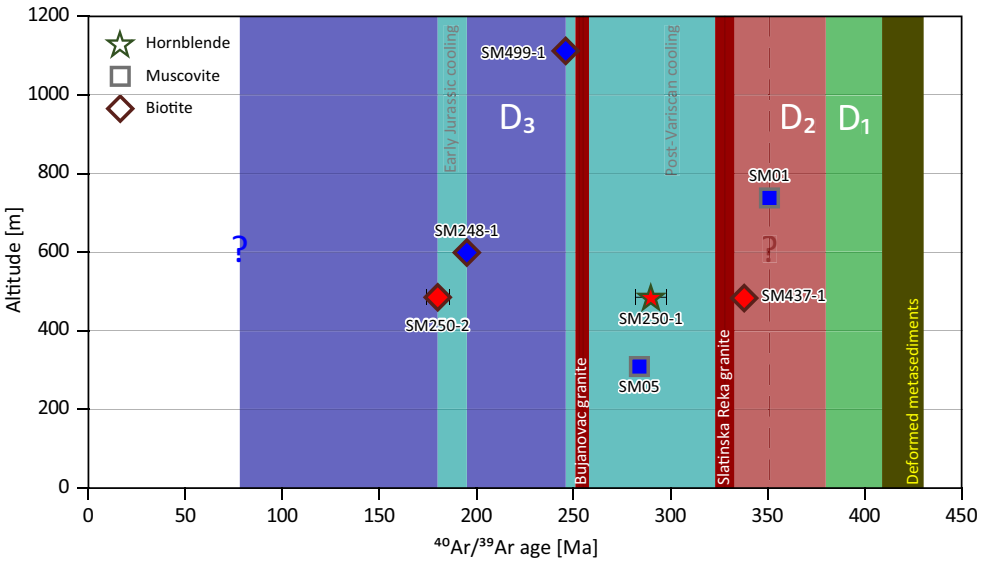

Fig. 16 Altitude versus $^{40}Ar/^{39}Ar$ dates of samples from this study. *Symbols with blue fill* represent plateau dates, whereas those with *red fill* represent weighted mean dates. Inferred durations of major deformation stages are given as *blue, red,* and *green* fields, whereas durations of thermal events are shown as fields in *light blue colour*. *Vertical bars* indicate indirect geological time constraints on duration of the deformation stages (in case of magmatic ages, the width of the *bar* represents 2σ uncertainty). See text for details

deformation, as the Gabrov Dol zone was formed under greenschist facies conditions and it unequivocally separates high-grade from lower-grade metamorphic rocks (Bonev et al. 1995; Gerdjikov et al. 2013).

Biotite from a mylonitic zone in the Vranjska Banja area with a top-to-the-south-west sense of shear (Figs. 3, 8d) yielded a disturbed pattern with an average $^{40}Ar/^{39}Ar$ date of 338 ± 2 Ma (SM437-1; Figs. 2, 14). The older muscovite $^{40}Ar/^{39}Ar$ plateau date in Vrvi Kobila area compared to the biotite date in Vranjska Banja area could be related to different closure temperatures of the two mineral phases (online Appendix A), which record regional cooling during the early Carboniferous. Although the $^{40}Ar/^{39}Ar$ data from the latter sample do not satisfy the criteria for a plateau date, it makes considerable geological sense that these two shear zones were both active during the deformation stage D_2.

Post-Variscan cooling

Early Permian cooling

An early Permian $^{40}Ar/^{39}Ar$ date of muscovite from the chlorite schists of Vlasina Unit south of Vlasotince (SM05; 284 ± 1 Ma; Table 1; Figs. 2, 14) is interpreted as the time of cooling below the greenschist facies conditions to which this area was exposed during the Variscan orogeny (Karamata and Krstić 1996; Graf 2001). Similar dates were obtained from a majority of the high-temperature heating steps in a disturbed $^{40}Ar/^{39}Ar$ date spectrum yielded by hornblende from the amphibolites in the Lower Complex west to south-west of the Vlajna magmatic complex (weighted mean date of 290 ± 8 Ma; SM250-1; Table 1; Figs. 2, 14). The elevated dates of higher temperature steps are almost certainly a result of excess ^{40}Ar. Late Carboniferous to early Permian $^{40}Ar/^{39}Ar$ dates of detrital white mica have been previously reported as a prominent population in the Mesozoic sedimentary rocks of the Dinarides of western Serbia (332–281 Ma; Ilic et al. 2005) and Struma Unit east of the study area (Fig. 2; Kounov 2002), confirming the regional extent of this cooling event. Similar long-lasting cooling and exhumation following the Variscan orogeny is already known in the Supragetic, Getic, and Danubian basement units of the South Carpathians (330–300 Ma; Fig. 2; Zagorchev 1980; Dallmeyer et al. 1998; Kounov 2002). Additionally, this time period corresponds to extensional tectonics reported throughout Europe resulting in the opening of fault-bound Stephanian–Permian sedimentary basins (Protić 1966; Maslarević and Krstić 1999; Yanev et al. 2001; McCann et al. 2006). Dallmeyer et al. (1998) report early Permian dextral strike-slip tectonics in Variscan Units of the Romanian South Carpathians. Therefore, the early Permian cooling in Vlasina Unit could have also taken place in a transtensional setting rather than a purely extensional one. Retention of older $^{40}Ar/^{39}Ar$ dates (samples SM01 and SM437-1; Table 1; Fig. 2) in central parts of the study area shows that this region had already cooled below ca. 310 °C (closure temperature of biotite; Harrison et al. 1985) during the early Carboniferous and was not affected by the early Permian extension and/or transtension. This area must have been juxtaposed to the vicinity of sample SM05 during strike-slip or compressional Alpine tectonics. Alternatively, it is possible that the entire central SMM had cooled down to temperatures below ca. 310 °C in Carboniferous, and only certain areas were reheated to temperatures above ca. 405 °C (closure temperature of muscovite; Harrison et al. 2009) during the early Permian rifting. In either case, the extent of unaffected and affected areas could not be exactly determined

due to low spatial resolution of thermochronological data. Deformational structures related to this tectonothermal stage in the study area were not recognised and the dated minerals belong to structures formed during Variscan tectonics.

Westward shear in Božica area

A relatively wide shear zone with top-to-the-west sense of shear formed within the Božica magmatic complex was recognised, although its exact regional extent and significance could not be evaluated. Mylonitic foliation is formed by clinozoisite and biotite with topotactic chlorite, suggesting that the shear zone was active under greenschist facies conditions. A biotite from this mylonite yielded an $^{40}Ar/^{39}Ar$ plateau date of 246 ± 1 Ma (SM499-1), representing a minimum time-constraint for activity along the shear zone (Table 1; Figs. 2, 14, 16). It must be noted that relicts of high-grade deformation (augen gneiss) have been observed in the Božica area, and its peak metamorphic conditions are somewhat higher (transitional high-greenschist to low-amphibolite facies) than in the majority of Vlasina Unit. Unfortunately, boundaries and exact relationship of the rocks in Božica area with the schists of Vlasina Unit could not be directly observed. A vast scatter in orientation of mineral lineation observed in this area potentially represents the effects of incomplete reworking of previous structures by the westward shearing event (Fig. 9c). Middle Triassic shearing in the Božica area closely postdates widespread extension along the European margin (ca. 250 Ma; De Wet et al. 1989; Himmerkus et al. 2009b; Peytcheva et al. 2009b) that eventually led to the opening of the Mesozoic Tethys west of the SMM (Robertson et al. 1991; Karamata and Krstić 1996; Pe-Piper 1998; Stampfli et al. 2002; Burg 2012). In western part of the central SMM, this extensional event is manifested by the Permo-Triassic granitic intrusion in the Bujanovac magmatic complex (Antić et al. 2015b). Therefore, this regional extensional event was most probably responsible for the formation of the shear zone in Božica area, whereas the evolution of this area since the end of Variscan orogeny until the Middle Triassic remains unresolved.

Third deformation stage D_3

Detailed structural investigations completed during the geological mapping of the central SMM in the 1970s provide evidence of kilometre-scale open folds in both the Lower Complex and the Vlasina Unit (Petrović 1969; Petrović et al. 1973; Vukanović et al. 1973, 1977; Babović et al. 1977). Statistical analysis of the structural data obtained during this study did not provide clear evidence of such a pattern, probably due to the relatively restricted number of observation points (e.g. Figs. 4, 9, 13a). However, foliation S_2 in western and central parts of the Lower Complex (Fig. 4a, b) possibly indicates orientation of limbs of a large-scale fold F_3. Additionally, scarce spaced and crenulation cleavage, subperpendicular or at a high angle to the earlier foliation S_2 (Fig. 12b), provides outcrop-scale evidence for a third deformation stage (D_3). Crenulation cleavage formed in the Early Triassic syn-metamorphic mylonites in the Božica magmatic complex (biotite $^{40}Ar/^{39}Ar$ plateau date 246 ± 1 Ma; SM499-1; Table 1; Fig. 14) provides a maximum age constraint on D_3 (Fig. 16). Minimum age constraint is given by zircon fission-track age from the orthogneiss of the Božica magmatic complex suggesting temperatures below 250 °C in the Late Cretaceous (Antić et al. 2015a).

Deformation in the Permo-Triassic Bujanovac pluton

The predominantly north-eastward dipping spaced cleavage and S–C fabric formed in the Permo-Triassic Bujanovac granite (U–Pb zircon ages of 255 ± 3 and 253 ± 2 Ma; Antić et al. 2015b) is clear evidence for Mesozoic ductile deformation (Figs. 10e, 13b). Due to a relatively small number of observations, these structures could not be clearly attributed to any of the deformation stages discussed above. The structural evidence for this deformation was not recognised farther away from the Bujanovac magmatic complex, probably due to generally low strain exerted during this event or the very low angle between the new cleavage S_c (Fig. 13c) and the older penetrative foliation S_2 (Fig. 4c). Likewise, the area affected by this deformation could not be clearly determined. Deformation of much higher intensity than that observed in Bujanovac granite has been reported in the Arnea granite in Greece (Kydonakis et al. 2015a). This granite is of similar age as Bujanovac (De Wet et al. 1989; Himmerkus et al. 2009b), and its deformation is reported to be related to Early Cretaceous south-westward thrusting.

Jurassic cooling

Evidence of retrogression of the mineral assemblages in the Lower Complex and the EVS is provided by the commonly observed replacement of K-feldspar by muscovite and sericite. No ductile deformation accompanied this retrogression. The Early Jurassic $^{40}Ar/^{39}Ar$ plateau date of biotite from gneiss west of the Vlajna magmatic complex in central parts of the Lower Complex (SM248-1; 195 ± 1 Ma; Table 1; Figs. 2, 14) suggests that some local reheating to temperatures above ca. 310 °C (closure temperature of biotite; online Appendix A) took place in Early Jurassic. During this local thermal event, which could explain the evidence of retrogression observed in

the Lower Complex gneisses (protolith U–Pb zircon age of 569 ± 9 Ma; Antić et al. 2015b), no ductile deformation occurred as the dated biotite forms foliation S_2 that was related to Variscan orogeny and shows no signs of subsequent recrystallisation. In this case, the $^{40}Ar/^{39}Ar$ plateau date of 195 ± 1 Ma represents cooling below temperatures that caused retrogression, thus setting a minimum age constraint on the low-grade overprint (Fig. 16). Although exhibiting a disturbed step-date spectrum, the Early Jurassic mean $^{40}Ar/^{39}Ar$ date of biotite from a Lower Complex gneiss west to south-west of Vlajna magmatic complex (182 ± 6 Ma; SM250-2; Table 1; Figs. 2, 14) highlights the regional importance of this thermal event. The low-grade overprint in Lower Complex of central SMM is probably contemporaneous to the greenschist metamorphism and deformation of Triassic sedimentary cover in north-western corner of the EVS (Novo Brdo schists; Pavić et al. 1983; Antić et al. 2015b). In this case, the Triassic age of sedimentary protoliths of Novo Brdo schists represents the maximum age constraint on the retrogression observed in the Lower Complex.

Previous Rb–Sr dating of biotite in Božica orthogneiss yielded dates of 166, 203, and 241 Ma (uncertainties not reported; Babović et al. 1977), which are interpreted as partial resetting of an original Permo-Triassic cooling age by the Jurassic low-grade event. Younger K–Ar cooling dates were previously reported for the whole-rock samples from the western part of the Lower Complex (137–122 Ma; Milovanović 1990) and mica from the same unit north of the study area (151–127 Ma; Balogh et al. 1994).

West of SMM (in present coordinates), the Early to Middle Jurassic intra-oceanic subduction of the Triassic Vardar ocean (Kostopoulos et al. 2001; Brown and Robertson 2003; Zachariadis 2007) led to opening of a supra-subduction-zone basin in Middle Jurassic (Channell and Kozur 1997; Božović et al. 2013). The effects of thermal convection in the mantle wedge on the overriding continental crust along with penetration of the dehydration fluids from the subducted slab of Vardar might have caused the initial thermal event, locally resetting the argon isotopic system of mica in gneisses of the Lower Complex. Alternatively, this thermal event could be related to shoulder extension and exhumation during the rifting stage of Ceahlău-Severin Ocean, which had completely opened in the Middle Jurassic (Dallmeyer et al. 1998; Iancu et al. 2005). However, given the lack of evidence of Ceahlău-Severin Ocean south of Kula Unit in north-western Bulgaria, the subduction of Vardar represents a more probable cause for the Jurassic thermal event in central SMM. General Early Jurassic hiatus in sedimentary sequences of Supragetic and Getic units in Serbia and Bulgaria may represent a further evidence for the regional exhumation and cooling at that time (e.g. Anđelković 1967; Tchoumatchenco 2006).

Although they share similar pre-Variscan evolution (Antić et al. 2015b), the Vertiskos unit in northern Greece and the Ograzhden Unit in south-western Bulgaria and eastern Macedonia, which are traditionally considered as parts of the SMM, show somewhat different Alpine evolution compared to the central SMM. After Variscan metamorphism (e.g. Zidarov et al. 2004, 2007; Peytcheva et al. 2005; Kounov et al. 2012), the rocks of Ograzhden Unit south-east of Kjustendil were brought to shallower crustal levels during Late Jurassic (muscovite $^{40}Ar/^{39}Ar$ mean date of ca. 160 Ma; Fig. 2; Kounov et al. 2010). The rocks of Vertiskos Unit were also initially metamorphosed during Variscan orogeny (Borsi et al. 1965; Kockel et al. 1977), whereas they have suffered local HP metamorphism during Early Jurassic (Reischmann and Kostopoulos 2001; Kydonakis et al. 2015b) followed by Barrovian metamorphism and intensive ductile deformation during Cretaceous, which almost completely reworked the older fabric (Dixon and Dimitriadis 1984; De Wet et al. 1989; Burg et al. 1995; Kilias et al. 1997, 1999; Kostopoulos et al. 2001; Kydonakis et al. 2015a).

Conclusions

Structural investigations provided evidence of at least three major stages of ductile deformation in the central SMM. Despite different peak metamorphic conditions in the Lower Complex and the Vlasina Unit, both units experienced a common deformational evolution. $^{40}Ar/^{39}Ar$ data helped refine the established deformational evolution and asses the regional importance of the determined tectonic events.

- The earliest stage of deformation D_1 in the central SMM is related to isoclinal folding, commonly preserved as decimetre-scale quartz–feldspar rootless fold hinges.
- The second deformation stage D_2 is associated with general south-eastward direction of tectonic transport and refolding of older structures into recumbent metre- to kilometre-scale tight to isoclinal folds.
- Deformation stages D_1 and D_2 could not be temporally separated and probably have taken place in close sequence. Based on the stratigraphic age of the youngest affected sediments, and the intrusion ages of the oldest undeformed magmatic rocks, the age of these two ductile deformation stages is constrained to the Variscan orogeny (i.e. ca. 408-ca. 328). During this time, the SMM was involved in a transpressional amalgamation of the western and eastern parts of the Galatian super-

terrane and subsequent collision with Laurussia, which could account for the changes in direction of strain axes during D_1 and D_2.

- A trend of diminishing strain and metamorphic grade from amphibolite facies in the Lower Complex, across greenschist facies in the pre-Ordovician Vlasina to anchimetamorphism in the post-Cambrian Vlasina suggests different crustal positions of the constituents of central SMM during the Variscan orogeny.
- Cooling below greenschist facies conditions in the western part of Vlasina Unit has taken place in a post-orogenic setting (extensional or transtensional) in early Permian (284 ± 1 Ma).
- The age of activity along top-to-the-west shear zone formed within orthogneiss in Božica area of the Vlasina Unit was constrained to Middle Triassic (246 ± 1 Ma). This age coincides with widespread extension related to the opening of the Mesozoic Tethys.
- Rare outcrop-scale evidence of the final stage of ductile deformation D_3 is limited to spaced and crenulation cleavage. These structures are probably related to the large-scale folding reported by earlier studies. The maximum age of this event is constrained by crenulation of the Middle Triassic mylonitic foliation in Božica area.
- Anastomosing shear zones, S–C fabric, and spaced cleavage developed in the Permo-Triassic Bujanovac granite provide evidence of an additional post-Triassic ductile deformation event. Additional data are needed to constrain the area affected by this deformation and its exact timing.
- A greenschist facies retrogression in the Lower Complex had probably occurred in Early Jurassic, and it is probably related to thermal processes in the overriding plate above subducting slab of the Mesozoic Tethys Ocean.

Acknowledgements Guilio Viola and Ianko Gerdjikov are gratefully acknowledged for their help on improving the overall quality of the manuscript. This study was financed through the Swiss National Science Foundation Grants (200021_125311 and 200020_14434) and a Grant from the Freiwillige Akademische Gesellschaft Basel. Constructive reviews by Nikolay Bonev and Neven Georgiev have helped to improve the quality of this paper.

References

Anđelković M (1967) Strukturno facijalne zone središnje i istočne Srbije. Zbornik Rudarsko-metalurškog fakulteta i Instituta za bakar 5

Anđelković M, Anđelković J (1995) Značaj Ilirske faze za geološki razvoj Moravida. Ann Géol Penins Balk 59:1–11

Antić MD, Kounov A, Trivić B et al (2015a) Alpine thermal events in the central Serbo-Macedonian Massif (southeastern Serbia). Int J Earth Sci (Geol Rundsch) 105:1485–1505. doi:10.1007/s00531-015-1266-z

Antić M, Peytcheva I, von Quadt A et al (2015b) Pre-Alpine evolution of a segment of the North-Gondwanan margin: geochronological and geochemical evidence from the central Serbo-Macedonian Massif. Gondwana Res. doi:10.1016/j.gr.2015.07.020

Babović M, Roglić Č, Avramović V, Marić S (1977) Tumač za list Trgovište sa Radomirom. Savezni Geološki Zavod, Belgrade

Balogh K, Svingor É, Cvetković V (1994) Ages and intensities of metamorphic processes in the Batočina area, Serbo-Macedonian massif. Acta Mineralogica-Petrographica XXXV:81–94

Banjac N (2004) Stratigrafija Srbije i Crne Gore. Rudarsko-geološki fakultet, Belgrade

Bastida F, Aller J, Fernández FJ et al (2014) Recumbent folds: key structural elements in orogenic belts. Earth-Sci Rev 135:162–183. doi:10.1016/j.earscirev.2014.05.002

Bonev K, Ivanov Z, Ricou L-E (1995) Dénudation tectonique au toit du noyau métamorphique Rhodopien-macédonien: la faille normale ductile de Gabrov Dol (Bulgarie). Bull Soc Géol France 166:47–55

Bonev N, Marchev P, Ovtcharova M et al (2010) U-Pb LA-ICP/MS zircon geochronology of metamorphic basement and Oligocene volcanic rocks from the SE Rhodopes: inferences for the geological history of the Eastern Rhodope crystalline basement. Bulgarian Geological Society, Sofia, pp 115–116

Bonev N, Marchev P, Moritz R, Collings D (2015) Jurassic subduction zone tectonics of the Rhodope Massif in the Thrace region (NE Greece) as revealed by new U-Pb and 40Ar/39Ar geochronology of the Evros ophiolite and high-grade basement rocks. Gondwana Res 27:760–775. doi:10.1016/j.gr.2014.08.008

Borsi S, Ferrara G, Mercier J (1965) Détermination de l'âge des séries métamorphiques du Massif Serbo-Macédonien au Nord-Est de Thessalonique (Grèce) par les méthodes Rb/Sr et K/Ar. Ann Soc Géol Nord 84:223–225

Bosse V, Boulvais P, Gautier P et al (2009) Fluid-induced disturbance of the monazite Th–Pb chronometer: in situ dating and element mapping in pegmatites from the Rhodope (Greece, Bulgaria). Chem Geol 261:286–302. doi:10.1016/j.chemgeo.2008.10.025

Božović M, Prelević D, Romer RL et al (2013) The Demir Kapija Ophiolite, Macedonia (FYROM): a snapshot of subduction initiation within a back-arc. J Petrol 54:1427–1453. doi:10.1093/petrology/egt017

Brown SAM, Robertson AHF (2003) Sedimentary geology as a key to understanding the tectonic evolution of the Mesozoic-Early Tertiary Paikon Massif, Vardar suture zone, N Greece. Sediment Geol 160:179–212. doi:10.1016/S0037-0738(02)00376-7

Burchfiel BC, Nakov R, Dumurdžanov N et al (2008) Evolution and dynamics of the Cenozoic tectonics of the South Balkan extensional system. Geosphere 4:919–938. doi:10.1130/GES00169.1

Burg J-P (1987) Regional shear variation in relation to diapirism and folding. J Struct Geol 9:925–934. doi:10.1016/0191-8141(87)90002-2

Burg J-P (2012) Rhodope: from Mesozoic convergence to Cenozoic extension. Review of petro-structural data in the geochronological frame. J Virtual Explor 42. doi:10.3809/jvirtex.2011.00270

Burg J-P, Godfriaux I, Ricou L-E (1995) Extension of the Mesozoic Rhodope thrust units in the Vertiskos-Kerdilion Massifs (Northern Greece). C R Acad Sci Paris 320:889–896

Carrigan CW, Mukasa SB, Haydoutov I, Kolcheva K (2005) Age of Variscan magmatism from the Balkan sector of the orogen, central Bulgaria. Lithos 82:125–147. doi:10.1016/j.lithos.2004.12.010

Channell JET, Kozur HW (1997) How many oceans? Meliata, Vardar and Pindos oceans in Mesozoic Alpine paleogeography. Geology 25:183–186. doi:10.1130/0091-7613(1997)025<0183:HMOMVA>2.3.CO;2

Cohen KM, Finney SC, Gibbard PL, Fan J (2013) The ICS international chronostratigraphic chart. Episodes 36:199–204

Csontos L, Vörös A (2004) Mesozoic plate tectonic reconstruction of the Carpathian region. Palaeogeogr Palaeocol 210:1–56. doi:10.1016/j.palaeo.2004.02.033

Cvetković V (1992) Petrology of the metamorphic rocks from the northern parts of the Serbo-macedonian massif in the Batočina area. Magistar thesis, Faculty of Mining and Geology

Dabovski C, Boyanov I, Khrischev K et al (2002) Structure and Alpine evolution of Bulgaria. Geol Balc 32:9–15

Dallmeyer RD, Neubauer F, Fritz H, Mocanu V (1998) Variscan vs. Alpine tectonothermal evolution of the Southern Carpathian orogen: constraints from $^{40}Ar/^{39}Ar$ ages. Tectonophysics 290:111–135. doi:10.1016/S0040-1951(98)00006-7

Dalrymple GB, Lanphere MA (1974) $^{40}Ar/^{39}Ar$ age spectra of some undisturbed terrestrial samples. Geochim Cosmochim Acta 38:715–738. doi:10.1016/0016-7037(74)90146-X

De Wet AP, Miller JA, Bickle MJ, Chapman HJ (1989) Geology and geochronology of the Arnea, Sithonia and Ouranopolis intrusions, Chalkidiki peninsula, northern Greece. Tectonophysics 161:65–79. doi:10.1016/0040-1951(89)90303-X

Deleon G (1969) Pregled rezultata određivanja apsolutne geološke starosti granitoidnih stena u Jugoslaviji. Radovi Instituta za geološko-rudarska istraživanja i ispitivanja nuklearnih i drugih mineralnih sirovina 6:165–180

Dimitrijević MD (1957) Struktura kristalastih terena između Slišana i Preševa. Referati, predavanja, diskusije. Savez geoloških društava Jugoslavije, Sarajevo

Dimitrijević MD (1958) Geološki sastav i struktura bujanovačkog granitskog masiva. Rasprave ZGGI NRS 3

Dimitrijević MD (1959) Osnovne karakteristike stuba Srpsko-makedonske mase. Abstracts Simposium SGD, Belgrade

Dimitrijević MD (1963) Sur l'âge du métamorphisme et des plissements dans la masse Serbo-macédonienne. Bulletin. Instytut Geologiczny, Warszawa, pp 339–347

Dimitrijević MD (1967) Some problems of crystalline schists in the Serbo-Macedonian Massif. Reports Serbian Geological Society, Belgrade, pp 59–67

Dimitrijević MD (1972) Variscijski metamorfizam u aksijalnom delu Balkanskog poluostrva (mogućnosti nove genetske interpretacije). Zapisnici SGD za 1971. godinu:115–124

Dimitrijević MD (1997) Geology of Yugoslavia. Geological Institute GEMINI, Belgrade

Dimitrijević MN, Dimitrijević MD (1987) The turbiditic basins of Serbia. Serbian Academy of Science and Arts, Belgrade

Dimitrijević MD, Drakulić N (1958) Kristalasti škriljci Jablanice. Zbornik radova RGF 6

Dimitrova E (1964) Petrologie des kristallinen Sockels des Osogovo Gebirges. Bulg Acad Sci Bull Geol Inst 13:99–110

Dixon JE, Dimitriadis S (1984) Metamorphosed ophiolitic rocks from the Serbo-Macedonian Massif, near Lake Volvi, Northeast Greece. Geol Soc SP 17:603–618. doi:10.1144/GSL.SP.1984.017.01.47

Fernández FJ, Aller J, Bastida F (2007) Kinematics of a kilometric recumbent fold: the Courel syncline (Iberian massif, NW Spain). J Struct Geol 29:1650–1664. doi:10.1016/j.jsg.2007.05.009

Fossen H (1993) Linear fabrics in the Bergsdalen Nappes, southwest Norway: implications for deformation history and fold development. Norsk Geol Tidsskr 73:95–108

Froitzheim N, Jahn-Awe S, Frei D et al (2014) Age and composition of meta-ophiolite from the Rhodope Middle Allochthon (Satovcha, Bulgaria): a test for the maximum-allochthony hypothesis of the Hellenides. Tectonics 33:2014TC003526. doi:10.1002/2014TC003526

Fügenschuh B, Schmid SM (2005) Age and significance of core complex formation in a very curved orogen: evidence from fission track studies in the South Carpathians (Romania). Tectonophysics 404:33–53. doi:10.1016/j.tecto.2005.03.019

Georgiev N, Froitzheim N, Cherneva Z et al (2016) Structure and U-Pb zircon geochronology of an Alpine nappe stack telescoped by extensional detachment faulting (Kulidzhik area, Eastern Rhodopes, Bulgaria). Int J Earth Sci (Geol Rundsch). doi:10.1007/s00531-016-1293-4

Gerdjikov I, Lazarova A, Balkanska E et al (2010a) A new model for the pre-Permian basement of the Central Stara Planina Mountain. Comptes Rendus de l'Académie bulgare des Sciences 63:1169–1176

Gerdjikov I, Ruffet G, Lazarova A et al (2010b) $^{40}Ar/^{39}Ar$ geochronologic constraints of a Variscan transpression in Central Stara Planina Mountain. Proc Bulg Geol Soc, Sofia, pp 109–110

Gerdjikov I, Lazarova A, Kounov A, Vangelov D (2013) High-grade metamorphic complexes in Bulgaria "St Ivan Rilski". Ann Univ Min Geol 56:47–52

Goscombe BD, Passchier CW, Hand M (2004) Boudinage classification: end-member boudin types and modified boudin structures. J Struct Geol 26:739–763. doi:10.1016/j.jsg.2003.08.015

Graf J (2001) Alpine tectonics in Western Bulgaria: Cretaceous compression of the Kraishte region and Cenozoic exhumation of the crystalline Osogovo–Lisets Complex. Ph.D., ETH Zürich

Grubić A, Ercegovac M (2002) Age of the Veles "Schistes Lustres" Formation from the Vardar Ocean. In: Proceedings of XVII congress of CBGA. VEDA, Bratislava, pp 66–68

Grubić A, Đoković I, Marović M, Branković M (1999) Srpsko-Makedonska masa ne postoji. Vesnik 49:1–14

Grubić A, Đoković I, Marović M, Branković M (2005) Problem tektonskog položaja kristalina Srpsko-Makedonske mase. Zapisnici SGD za 1998, 1999, 2000, 2001, 2002 i 2003. Godinu 35–39

Harrison TM, Duncan I, McDougall I (1985) Diffusion of ^{40}Ar in biotite: temperature, pressure and compositional effects. Geochim Cosmochim Acta 49:2461–2468. doi:10.1016/0016-7037(85)90246-7

Harrison TM, Célérier J, Aikman AB et al (2009) Diffusion of ^{40}Ar in muscovite. Geochim Cosmochim Acta 73:1039–1051. doi:10.1016/j.gca.2008.09.038

Himmerkus F, Reischmann T, Kostopoulos D (2006) Late Proterozoic and Silurian basement units within the Serbo-Macedonian Massif, northern Greece: the significance of terrane accretion in the Hellenides. Geol Soc Spl Publ 260:35–50. doi:10.1144/GSL.SP.2006.260.01.03

Himmerkus F, Reischmann T, Kostopoulos D (2009a) Triassic rift-related meta-granites in the Internal Hellenides, Greece. Geol Mag 146:252. doi:10.1017/S001675680800592X

Himmerkus F, Reischmann T, Kostopoulos D (2009b) Serbo-Macedonian revisited: a Silurian basement terrane from northern Gondwana in the Internal Hellenides, Greece. Tectonophysics 473:20–35. doi:10.1016/j.tecto.2008.10.016

Himmerkus F, Zachariadis P, Reischmann T, Kostopoulos D (2011) The basement of the Mount Athos peninsula, northern Greece: insights from geochemistry and zircon ages. Int J Earth Sci (Geol Rundsch) 101:1467–1485. doi:10.1007/s00531-011-0644-4

Iancu V, Màruntiu M, Johan V, Ledru P (1998) High-grade metamorphic rocks in the pre-Alpine nappe stack of the Getic-Supragetic basement (Median Dacides, South Carpathians, Romania). Mineral Petrol 63:173–198. doi:10.1007/BF01164150

Iancu V, Berza T, Seghedi A et al (2005) Alpine polyphase tectono-metamorphic evolution of the South Carpathians: a new overview. Tectonophysics 410:337–365. doi:10.1016/j.tecto.2004.12.038

Ilic A, Neubauer F, Handler R (2005) Late Paleozoic-Mesozoic tectonics of the Dinarides revisited: implications from $^{40}Ar/^{39}Ar$ dating of detrital white micas. Geology 33:233–236. doi:10.1130/G20979.1

Ivanova P, Zidarov N (2011) Metamorphic evolution of spinel clinopyroxenites with clinopyroxene megacrysts from Ograzhden Mountain, SW Bulgaria. Proc Bulg Geol Soc, Sofia, pp 61–62

Jahn-Awe S, Froitzheim N, Nagel TJ et al (2010) Structural and geochronological evidence for Paleogene thrusting in the western Rhodopes, SW Bulgaria: elements for a new tectonic model of the Rhodope Metamorphic Province. Tectonics 29:TC3008. doi:10.1029/2009TC002558

Jahn-Awe S, Pleuger J, Frei D et al (2012) Time constraints for low-angle shear zones in the Central Rhodopes (Bulgaria) and their significance for the exhumation of high-pressure rocks. Int J Earth Sci (Geol Rundsch) 101:1971–2004. doi:10.1007/s00531-012-0764-5

Karamata S (2006) The geological development of the Balkan Peninsula related to the approach, collision and compression of Gondwanan and Eurasian units. Geol Soc Spl Publ 260:155–178. doi:10.1144/GSL.SP.2006.260.01.07

Karamata S, Krstić B (1996) Terranes of Serbia and neighbouring areas. In: Knežević-Đorđević V, Krstić B (eds) Terranes of Serbia. Faculty of Mining and Geology, University of Belgrade, Belgrade, pp 25–40

Karamata S, Stojanov R, Serafimovski T et al (1992) Tertiary magmatism in the Dinarides of the Vardar zone and the Serbo-Macedonian Massif. Geol Maced 6:127–186

Kilias A, Falalakis G, Mountrakis D (1997) Alpine tectonometamorphic history of the Serbomacedonian metamorphic rocks: implication for the tertiary unroofing of the Serbomacedonian-Rhodope metamorphic complexes (Makedonia, Greece). Ορυκτός Πλούτος 105:32–50

Kilias A, Falalakis G, Mountrakis D (1999) Cretaceous-tertiary structures and kinematics of the Serbomacedonian metamorphic rocks and their relation to the exhumation of the Hellenic hinterland (Macedonia, Greece). Int J Earth Sci (Geol Rundsch) 88:513–531. doi:10.1007/s005310050282

Kockel F, Mollat H, Walther HW (1971) Geologie der Serbo-Mazedonischen Massivs und seines mesozoischen Rahmens (Nordgriechenland). Geol Jahrb 89:529–551

Kockel F, Mollat H, Walther HW (1977) Erläuterungen zur Geologischen Karte der Chalkidiki und angrenzender Gebiete 1:100000 (Nord-Griechenland). Bundesanstalt für Geowissenschaften und Rohstoffe, Hannover

Korikovsky S, Karamata S, Milovanović D (2003) Retrograted kyanite eclogites and eclogittized gabbro-norites of the Serbomacedonian unit. Central Serbia, reaction textures and geothermobarometry. Zbornik abstraktov. Bratislava, pp 13–14

Kostopoulos D, Reischmann T, Sklavounos S (2001) Palaeozoic and early Mesozoic magmatism and metamorphism in the Serbo-Macedonian massif, Central Macedonia, Northern Greece. Abstracts. Cambridge Publications, Strasbourg, p 318

Kounov A (2002) Thermotectonic evolution of Kraishte, western Bulgaria. Ph.D., ETH Zürich

Kounov A, Seward D, Bernoulli D et al (2004) Thermotectonic evolution of an extensional dome: the Cenozoic Osogovo-Lisets core complex (Kraishte zone, western Bulgaria). Int J Earth Sci (Geol Rundsch) 93:1008–1024. doi:10.1007/s00531-004-0435-2

Kounov A, Seward D, Burg J-P et al (2010) Geochronological and structural constraints on the Cretaceous thermotectonic evolution of the Kraishte zone, western Bulgaria. Tectonics 29:TC2002. doi:10.1029/2009TC002509

Kounov A, Burg J-P, Bernoulli D et al (2011) Paleostress analysis of Cenozoic faulting in the Kraishte area, SW Bulgaria. J Struct Geol 33:859–874. doi:10.1016/j.jsg.2011.03.006

Kounov A, Graf J, von Quadt A et al (2012) Evidence for a "Cadomian" ophiolite and magmatic-arc complex in SW Bulgaria. Precambr Res 212–213:275–295. doi:10.1016/j.precamres.2012.06.003

Kräutner HG, Krstić B (2002) Alpine and pre-Alpine structural units within the southern Carpathians and eastern Balkanides. In: Proceedings of XVII congress of CBGA. VEDA, Bratislava

Krstić N, Karamata S (1992) Terani u Karpato-Balkanidima istočne Srbije. Zapisnici SGD jubilarna knjiga 1891–1991:57–69

Krstić B, Maslarević L, Ercegovac M, Đajić S (2002) Devonian of the Serbian Carpatho-Balkanides. In: Proceedings of XVII congress of CBGA. VEDA, Bratislava

Kydonakis K, Gallagher K, Brun J-P et al (2014) Upper Cretaceous exhumation of the western Rhodope Metamorphic Province (Chalkidiki Peninsula, northern Greece). Tectonics 33:2014TC003572. doi:10.1002/2014TC003572

Kydonakis K, Brun J-P, Sokoutis D, Gueydan F (2015a) Kinematics of Cretaceous subduction and exhumation in the western Rhodope (Chalkidiki block). Tectonophysics 665:218–235. doi:10.1016/j.tecto.2015.09.034

Kydonakis K, Moulas E, Chatzitheodoridis E et al (2015b) First-report on Mesozoic eclogite-facies metamorphism preceding Barrovian overprint from the western Rhodope (Chalkidiki, northern Greece). Lithos 220–223:147–163. doi:10.1016/j.lithos.2015.02.007

Lakova I (2009) Acritarch evidence on Silurian age of the low-grade metamorphic Palaeozoic rocks in the Kraishte area (Morava Unit). Rev Bulg Geol Soc 70:23–30

Liati A (2005) Identification of repeated Alpine (ultra) high-pressure metamorphic events by U-Pb SHRIMP geochronology and REE geochemistry of zircon: the Rhodope zone of Northern Greece. Contrib Miner Petrol 150:608–630. doi:10.1007/s00410-005-0038-3

Lilov P, Zagorchev IS (1993) K-Ar data for the deformation and low-grade metamorphism in Permian and Triassic red beds in SW Bulgaria. Geol Balc 23:46

Macheva L, Titorenkova R, Zidarov N (2005) Kyanite-staurolite-garnet orthoschists. Central Laboratory of Mineralogy and Crystallography "Acad. Ivan Kostov, Sofia

Malešević M, Vukanović M, Obradinović Z et al (1980) Tumač za list Kuršumlija. Savezni Geološki Zavod, Belgrade

Marinova R, Grozdev V, Ivanova D et al (2010) List Tsarvena Jabuka, Vlasotince, Tran-North and Tran-South. Ministry of Environment and Water, Bulgarian National Geological Survey, Sofia

Marović M, Toljić M, Rundić L, Milivojević J (2007) Neoalpine tectonics of Serbia. Serbian Geological Society, Belgrade

Maslarević L, Krstić B (1999) Permian continental redbeds of the Serbian South-Carpathian and Balkan (Stara Planina) Mountains. Abstracts. Brescia, pp 92–64

Matenco L, Schmid S (1999) Exhumation of the Danubian nappes system (South Carpathians) during the Early Tertiary: inferences from kinematic and paleostress analysis at the Getic/Danubian nappes contact. Tectonophysics 314:401–422. doi:10.1016/S0040-1951(99)00221-8

McCann T, Pascal C, Timmerman MJ et al (2006) Post-Variscan (end Carboniferous-Early Permian) basin evolution in Western and Central Europe. Geol Soc Mem 32:355–388. doi:10.1144/GSL.MEM.2006.032.01.22

Meinhold G, Kostopoulos D, Frei D et al (2010) U-Pb LA-SF-ICP-MS zircon geochronology of the Serbo-Macedonian Massif, Greece: palaeotectonic constraints for Gondwana-derived terranes in the Eastern Mediterranean. Int J Earth Sci (Geol Rundsch) 99:813–832. doi:10.1007/s00531-009-0425-5

Mihailescu N, Dimitrijević MD, Dimitrijević MN (1967) Les fossiles dans le flysch. Reports. Serbian Geological Society, Belgrade, pp 371–378

Milovanović D (1989) Metamorphism of the Serbo-Macedonian massif. In: Proceedings of 28th international geological congress, Washington, pp 439–441

Milovanović D (1990) Petrologija gnajseva Srpsko-makedonske mase u području između Tulara i Lebana. In: Proceedings of the XII

congress of the geologists of Yugoslavia. Prosveta, Ohrid, pp 310–321
Milovanović D (1992) Amfibolske stene u području između Medveđe i Lebana. Ann Géol Penins Balk 56:253–268
Milovanović D, Milovanović M, Oberhänsli R (1988) Petrology of green-rocks of the Vlasina complex in the Manastiriška river area (Vlasotince). Vesnik 44:101–128
Mladenović A, Trivić B, Antić M et al (2014) The recent fault kinematics in the westernmost part of the Getic nappe system (Eastern Serbia): evidence from fault slip and focal mechanism data. Geol Carpath 65:147–161. doi:10.2478/geoca-2014-0010
Mukasa SB, Haydoutov I, Carrigan CW, Kolcheva K (2003) Thermobarometry and $^{40}Ar/^{39}Ar$ ages of eclogitic and gneissic rocks in the Sredna Gora and Rhodope terranes of Bulgaria. J Czech Geol Soc 48:94–95
Nenova P, Zidarov N (2008) Eclogites from Maleshevska Mountain, SW Bulgaria. Central Laboratory of Mineralogy and Crystallography "Acad. Ivan Kostov", Sofia
Neubauer F (2002) Evolution of late Neoproterozoic to early Paleozoic tectonic elements in Central and Southeast European Alpine mountain belts: review and synthesis. Tectonophysics 352:87–103. doi:10.1016/S0040-1951(02)00190-7
Pantić N, Dimitrijević MD, Hercegovac M (1967) Mikrofloristički podaci o starosti Vlasinskog kompleksa. Zapisnici SGD za 1966. godinu
Passchier CW, den Brok SWI, van Gool JAM et al (1997) A laterally constricted shear zone system—the Nordre Strømfjord steep belt, Nagssugtoqidian Orogen, W. Greenland. Terra Nova 9:199–202. doi:10.1111/j.1365-3121.1997.tb00012.x
Pavić A, Menković L, Košćal M (1983) Tumač za list Uroševac. Savezni Geološki Zavod, Belgrade
Pavlović P (1962) O nekim ordovicijskim inartikulatnim brahiopodima u metamorfnim stenama kod Bosiljgrada (Jugoistočna Srbija) i o značaju ovog nalaska. Ann Géol Penins Balk 39:99–112
Pavlović P (1977) O "Gornjem (Vlasinskom) kompleksu" i podeli metamorfnih stena Srpsko-Makedonskog metamorfnog terena. Zapisnici SGD za 1975. i 1976. Godinu 123–132
Pe-Piper G (1998) The nature of Triassic extension-related magmatism in Greece; evidence from Nd and Pb isotope geochemistry. Geol Mag 135:331–348
Petković V (1930) O tektonskom sklopu istočne Srbije. Glas Srpske kraljevske akademije 140:151–188
Petrović BS (1969) The structure of the Vlasina Crystalline Complex in the broad area of Crna Trava. Rudarsko-geološki fakultet, Belgrade
Petrović B S, Karamata S (1965) Metaklastiti—baza gornjeg kompleksa kristalastih škriljaca SMM. In: Proceedings of the 7th congress of the geologists of Yugoslavia, Zagreb
Petrović B, Dimitrijević MD, Karamata S (1973) Tumač za list Vlasotince. Savezni Geološki Zavod, Belgrade
Peytcheva I, von Quadt A, Ovtcharova M et al (2004) Metagranitoids from the eastern part of the Central Rhodopean Dome (Bulgaria): U-Pb, Rb–Sr and $^{40}Ar/^{39}Ar$ timing of emplacement and exhumation and isotope-geochemical features. Miner Petrol 82:1–31. doi:10.1007/s00710-004-0039-3
Peytcheva I, von Quadt A, Titorenkova R, et al (2005) Skrut granitoids from Belassitsa Mountain, SW Bulgaria: constraints from isotope geochronological and geochemical zircon data. In: Proceedings of Bulgarian Geological Society, Sofia, pp 205–208
Peytcheva I, von Quadt A, Sarov S et al (2009a) U-Pb LA-ICP/MS zircon geochronology of metamorphic basement and Oligocene volcanic rocks from the SE Rhodopes: inferences for the geological history of the Eastern Rhodope crystalline basement. Bul Geol Soc, Sofia, pp 17–18
Peytcheva I, von Quadt A, Tarassov M et al (2009b) Timing of Igralishte pluton in Ograzhden Mountain, SW Bulgaria: implications for the tectono-magmatic evolution of the region. Geol Balc 38:5–14
Plissart G, Diot H, Monnier C et al (2012) Relationship between a syntectonic granitic intrusion and a shear zone in the Southern Carpathian-Balkan area (Almăj Mountains, Romania): implications for late Variscan kinematics and Cherbelezu granitoid emplacement. J Struct Geol 39:83–102. doi:10.1016/j.jsg.2012.03.004
Popović R (1991) Srpsko-Makedonska masa ili Pelagonsko-Rodopski i Moravski masiv. Radovi Geoinstituta 25:7–20
Popović R (1995) Srpsko-Makedonska masa: da ili ne? Zapisnici SGD za 1990. i 1991. Godinu 59–61
Protić M (1966) Permski crveni peščari istočne Srbije—sredine njihovog stvaranja. Referati VI savetovanja geologa SFRJ, Ohrid
Reischmann T, Kostopoulos D (2001) Geochronology and P-T constraints on the exhumation history of an UHP eclogite from Northern Greece. Abstracts. Eos Trans AGU, San Francisco, p 0987
Ricou L-E (1994) Tethys reconstructed: plates, continental fragments and their boundaries since 260 Ma from Central America to South-eastern Asia. Geodin Acta 7:169–218. doi:10.1080/09853111.1994.11105266
Ricou L-E, Burg J-P, Godfriaux I, Ivanov Z (1998) Rhodope and Vardar: the metamorphic and the olistostromic paired belts related to the Cretaceous subduction under Europe. Geodin Acta 11:285–309. doi:10.1016/S0985-3111(99)80018-7
Robertson AHF, Clift PD, Degnan PJ, Jones G (1991) Palaeogeographic and palaeotectonic evolution of the Eastern Mediterranean Neotethys. Palaeogeogr Palaeocol 87:289–343. doi:10.1016/0031-0182(91)90140-M
Robertson A, Karamata S, Šarić K (2009) Overview of ophiolites and related units in the Late Palaeozoic-Early Cenozoic magmatic and tectonic development of Tethys in the northern part of the Balkan region. Lithos 108:1–36. doi:10.1016/j.lithos.2008.09.007
Săndulescu M (1984) Geotectonica Romaniei. Editura Tehnică, Bucharest
Schmid SM, Bernoulli D, Fügenschuh B et al (2008) The Alpine-Carpathian-Dinaridic orogenic system: correlation and evolution of tectonic units. Swiss J Geosci 101:139–183. doi:10.1007/s00015-008-1247-3
Simpson C, Wintsch RP (1989) Evidence for deformation-induced K-feldspar replacement by myrmekite. J Metamorph Geol 7:261–275. doi:10.1111/j.1525-1314.1989.tb00588.x
Spassov C (1973) Stratigraphie des Devons in Sudwest-Bulgarien. Bull Geol Inst 22:5–38
Stampfli GM, Hochard C (2009) Plate tectonics of the Alpine realm. Geol Soc Spl Publ 327:89–111. doi:10.1144/SP327.6
Stampfli GM, von Raumer JF, Borel GD (2002) Paleozoic evolution of pre-Variscan terranes: from Gondwana to the Variscan collision. Geol Soc Am Spl Pap 364:263–280. doi:10.1130/0-8137-2364-7.263
Stampfli GM, Hochard C, Vérard C et al (2013) The formation of Pangea. Tectonophysics 593:1–19. doi:10.1016/j.tecto.2013.02.037
Stipp M, Stünitz H, Heilbronner R, Schmid SM (2002) The eastern Tonale fault zone: a "natural laboratory" for crystal plastic deformation of quartz over a temperature range from 250 to 700 °C. J Struct Geol 24:1861–1884. doi:10.1016/S0191-8141(02)00035-4
Stojadinovic U, Matenco L, Andriessen PAM et al (2013) The balance between orogenic building and subsequent extension during the tertiary evolution of the NE Dinarides: constraints from low-temperature thermochronology. Glob Planet Change 103:19–38. doi:10.1016/j.gloplacha.2012.08.004
Tchoumatchenco P (2006) Jurassic tectonics of Bulgaria and the adjacent areas. Rev Bulg Geol Soc 67:86–103

Tobisch OT, Paterson SR (1988) Analysis and interpretation of composite foliations in areas of progressive deformation. J Struct Geol 10:745–754. doi:10.1016/0191-8141(88)90081-8

Toljić M, Matenco L, Ducea MN et al (2013) The evolution of a key segment in the Europe-Adria collision: the Fruška Gora of northern Serbia. Glob Planet Change 103:39–62. doi:10.1016/j.gloplacha.2012.10.009

Tranos MD, Lacombe O (2014) Late Cenozoic faulting in SW Bulgaria: fault geometry, kinematics and driving stress regimes. Implications for late orogenic processes in the Hellenic hinterland. J Geodyn 74:32–55. doi:10.1016/j.jog.2013.12.001

Turpaud P, Reischmann T (2010) Characterisation of igneous terranes by zircon dating: implications for UHP occurrences and suture identification in the Central Rhodope, northern Greece. Int J Earth Sci (Geol Rundsch) 99:567–591. doi:10.1007/s00531-008-0409-x

Ustaszewski K, Schmid SM, Lugović B et al (2009) Late Cretaceous intra-oceanic magmatism in the internal Dinarides (northern Bosnia and Herzegovina): implications for the collision of the Adriatic and European plates. Lithos 108:106–125. doi:10.1016/j.lithos.2008.09.010

van Hinsbergen DJJ, Schmid SM (2012) Map view restoration of Aegean-West Anatolian accretion and extension since the Eocene. Tectonics 31:TC5005. doi:10.1029/2012TC003132

Vasković N (1998) P-T condition of the mica schists from the Vranjska Banja Series. In: Proceedings of the XIII congress of the geologists of Yugoslavia. Herceg Novi, pp 41–59

Vasković N (2002) Petrology and P-T condition of white mica-chlorite schists from Vlasina series—Surdulica, SE Serbia. Ann Géol Penins Balk. doi:10.2298/GABP0264199V

Vasković N, Matović V, Srećković-Batoćanin D (2003) Petrology of garnet-amphibolite with White Mica from Vranjska Banja Series (Serbian-Macedonian Massif, SE Serbia). Studia Universitatis Babeş-Bolyai 128–133

von Raumer JF, Stampfli GM, Bussy F (2003) Gondwana-derived microcontinents—the constituents of the Variscan and Alpine collisional orogens. Tectonophysics 365:7–22. doi:10.1016/S0040-1951(03)00015-5

von Raumer JF, Bussy F, Schaltegger U et al (2013) Pre-Mesozoic Alpine basements—their place in the European Paleozoic framework. Geol Soc Am Bull 125:89–108. doi:10.1130/B30654.1

Vujanović V, Cvetić S, Teofilović M (1974) Poreklo gnajseva Srbije i Makedonije. Zapisnici SGD za 1973. Godinu 266–270

Vukanović M, Karajičić L, Dimitrijević MD et al (1973) Tumač za list Leskovac. Savezni Geološki Zavod, Belgrade

Vukanović M, Dimitrijević MD, Dimitrijević M et al (1977) Tumač za list Vranje. Savezni Geološki Zavod, Belgrade

Vukanović M, Dimitrijević M, Dimitrijević MD et al (1982) Tumač za list Podujevo. Savezni Geološki Zavod, Belgrade

Whitney DL, Evans BW (2010) Abbreviations for names of rock-forming minerals. Am Miner 95:185–187. doi:10.2138/am.2010.3371

Yanev S, Popa M, Seghedi A, Oaie G (2001) Overview of the continental Permian deposits of Bulgaria and Romania. Nat Bresciana 25:269–279

Zachariadis P (2007) Ophiolites of the eastern Vardar Zone, N. Greece. Johannes Gutenberg Universität

Zagorčev IS, Bončeva I (1988) Indications of Devonian basic volcanism in Southwest Bulgaria. Geol Balc 18:55–63

Zagorchev IS (1980) Early Alpine deformations in the red beds within the Poletinci-Skrino fault zone. 1. Litostratigraphic features in light of structural studies. Geol Balc 10:37–60

Zagorchev IS (1981) Early Alpine deformations in the red beds within the Poletinci-Skrino fault zone. 2. Structure and deformations in the northern parts of the Vlahina block. Geol Balc 11:101–126

Zagorchev IS (1984) Pre-Alpine structure of South-west Bulgaria. In: Zagorchev IS, Mankov S, Bozkov I (eds) Problems of the geology of Southwestern Bulgaria. Tehnika, Sofia, pp 9–20

Zagorchev IS (1985) Deformation during the first stage of the Alpine Orogeny in the Skrino-Poletintsi faulted zone; IV Shipochan Anticline. Rev Bulg Geol Soc 46:287–298

Zagorchev IS, Milovanović D (2006) Deformations and metamorphism in the eastern parts of the Serbo-Macedonian Massif. In: Proceedings of Serbian Geological Society, Belgrade, pp 670–673

Zagorchev IS, Ruseva M (1982) Nappe structure of the southern parts of Osogovo Mts and the Pijanec region (SW Bulgaria). Geol Balc 12:35–57

Zagortchev IS (1993) Alpine evolution of the pre-Alpine amphibolite-facies basement in South Bulgaria. Mitteilungen der Österreichischen Geologischen Gesellschaft 86:9–21

Zelic M, Levi N, Malasoma A et al (2010) Alpine tectono-metamorphic history of the continental units from Vardar zone: the Kopaonik Metamorphic Complex (Dinaric-Hellenic belt, Serbia). Geol J 45:59–77. doi:10.1002/gj.1169

Zidarov N, Peytcheva I, von Quadt A (2003a) Mineral-petrological, geochemical and isotope studies of geological units in Serbo-Macedonian Massif, SW Bulgaria. Central Laboratory of Mineralogy and Crystallography "Acad. Ivan Kostov", Sofia

Zidarov N, Peytcheva I, von Quadt A, et al (2003b) Timing and magma sources of metagranites from the Serbo-Macedonian Massif (Ograzhden and Maleshavska Mountains, SW Bulgaria): constraints from UPb and Hf-Zircon and Sr whole rock isotope studies. In: Proceedings of Bulgarian Geological Society, Sofia, pp 89–91

Zidarov N, Peytcheva I, von Quadt A et al (2004) Timing and magma sources of Igralishte Pluton (SW Bulgaria): preliminary isotope-geochronological and geochemical data. In: Proceedings of Bulgarian Geological Society, Sofia

Zidarov N, Tarassova E, Peytcheva I et al (2007) Petrology, geochemistry and age dating of Skrut granitoids—new evidence for Early Triassic magmatism in Belasitsa Mountain (SW Bulgaria). Geol Balc 36:17–29